2.0 Physical Environment

2.1 Geology

Throughout most of the Precambrian the island of Newfoundland did not exist. Its development began around 620 million years ago with a geologic process known as the "Wilson Cycle" involving rifting, drifting, and ultimate collision of continental and oceanic crust. Extreme compressive forces resulting from colliding crustal plates formed the structurally elevated, folded and faulted landmass of the Appalachians in western Newfoundland, and accumulated onto it three other crustal fragments to the east that now make up the remainder of the island and its continental margin. The Appalachian orogen (mountain building process), as expressed in Newfoundland's geology, is the Paleozoic composite of three separate tectonic compressive events: the Taconic orogeny (during the Middle to Late Ordovician), the Salinic orogeny (Silurian), and the Late Devonian Acadian orogeny. These deformational events have left as their legacy the four distinct geological zones that now make up this island, which from west to east are the Humber, Dunnage, Gander, and Avalon zones (Figure 2.1) (Williams 1995a,b,c,d).

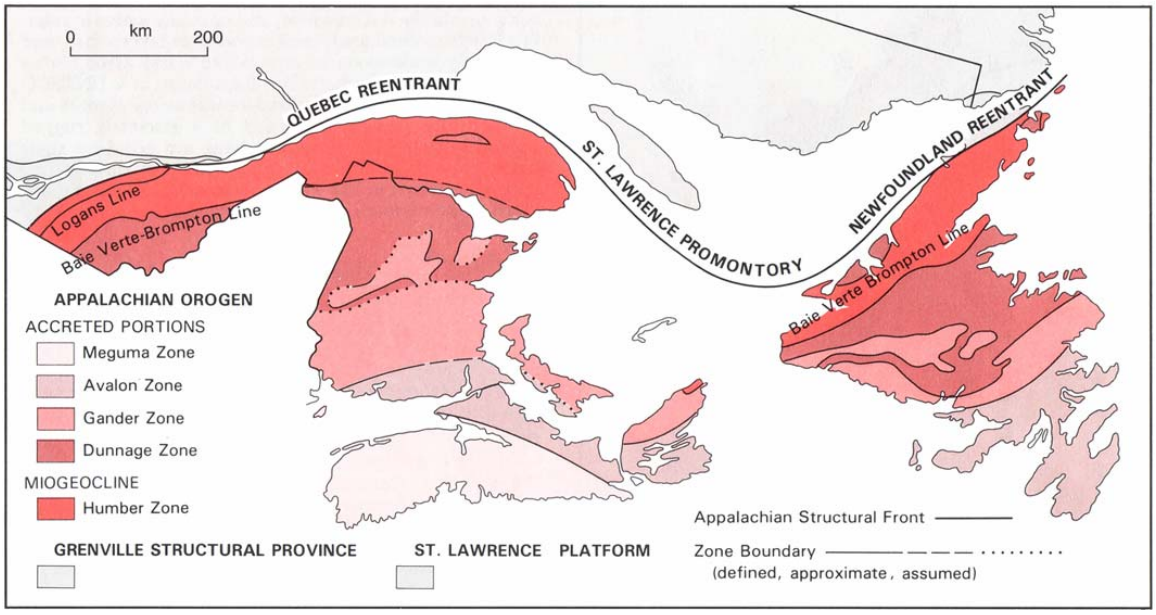

Figure 2.1. Simple Zonation of the Canadian Appalachian Region (adapted from Williams 1995a).

Newfoundland's geology is dynamic, and constantly evolving, with no internal temporal and spatial reference point. Thus, it is useful to view Newfoundland and its offshore areas from the interior, relatively stable, primordial continental crust of North America. It is upon this basement that younger rocks were laid down, reworked, and structurally telescoped by sedimentary processes, tectonic forces,

igneous activity, and metamorphism to form what is termed "the Humber zone". And it is to this zone that the three other crustal fragments were added by compressional tectonism, and later reshaped by sedimentary processes, igneous activity, and tensional forces to create the island of Newfoundland and its offshore areas as recognized today (Williams 1995b,c; Sandford 1993a,b).

Despite its complexities, Newfoundland's geology serves as one of the best records of the Appalachians and allows a clearer understanding of the geology of other parts of this mountain system, which can be traced for almost 10,000 km (Williams 1995a). Gros Morne National Park in western Newfoundland was declared a UNESCO World Heritage Site in 1987 mainly because of its rocks and geological relationships.

2.1.1 The Humber Zone – Laurentia's Ancient Continental Margin Affected by Appalachian Tectonism

Starting in the Precambrian with continental crust of the ancient North American continent, Laurentia, subaerial erosion exposed wide areas of this crust within the interior part of northern Canada, which is referred to interchangeably here as the Canadian Shield, continental basement, or craton. It includes the Superior Province underlying a large portion of Ontario and Quebec, and the Grenville Province along the eastern margin (Figure 2.2). This ancient craton developed a series of structural highs (arches) and lows (basins), which greatly influenced sedimentary processes along Laurentia's eastern margin. Being exposed to the effects of weathering and erosion, cratonic arches were the source of sediments that were transported by water and deposited within submerged areas of nearby basins. Along the margin of eastern Quebec and southern Labrador, sediments derived from the Beauge and Laurentian Arches were deposited upon crustal basement in the Anticosti Basin (Figure 2.3) during the Paleozoic, which contributed greatly to the development of the Eastern St Lawrence Platform. It is within sedimentary rocks of this ancient platform that are found hydrocarbon source and reservoir rocks of the Study Area (Sandford 1993a,b).

Early Cambrian to Middle Ordovician sedimentary rocks of the Humber zone of western Newfoundland provide an excellent record of the Eastern St. Lawrence Platform sediments. Phrased differently, the Humber zone comprises the Appalachian miogeocline: the ancient continental margin (platform sediments and underlying Grenvillian basement) that has been affected by Appalachian tectonism. The Appalachian Structural Front marks the western limit of the Humber zone and separates deformed rocks of the ancient margin from those that have been unaffected by orogeny (Figure 2.4). To the east of the Humber zone miogeocline are the accreted portions of the Appalachian orogen, rocks of the Dunnage, Gander, and Avalon zones. Their geographic provenances are not as well understood as that of the Humber zone, but these rocks are thought to represent oceanic crust (i.e., the Dunnage zone) underlying the Paleozoic Iapetus ocean that bordered Laurentia, continental margin (i.e., the Gander zone) on the eastern rim of the Iapetus, and a continental crustal segment (i.e., the Avalon zone) that later remained attached to North America as the Mesozoic Atlantic Ocean developed to the east of Newfoundland's present continental margin (Williams 1995a,b,c,d,e,f; Greenough 1995; Erdmer and Williams 1995).

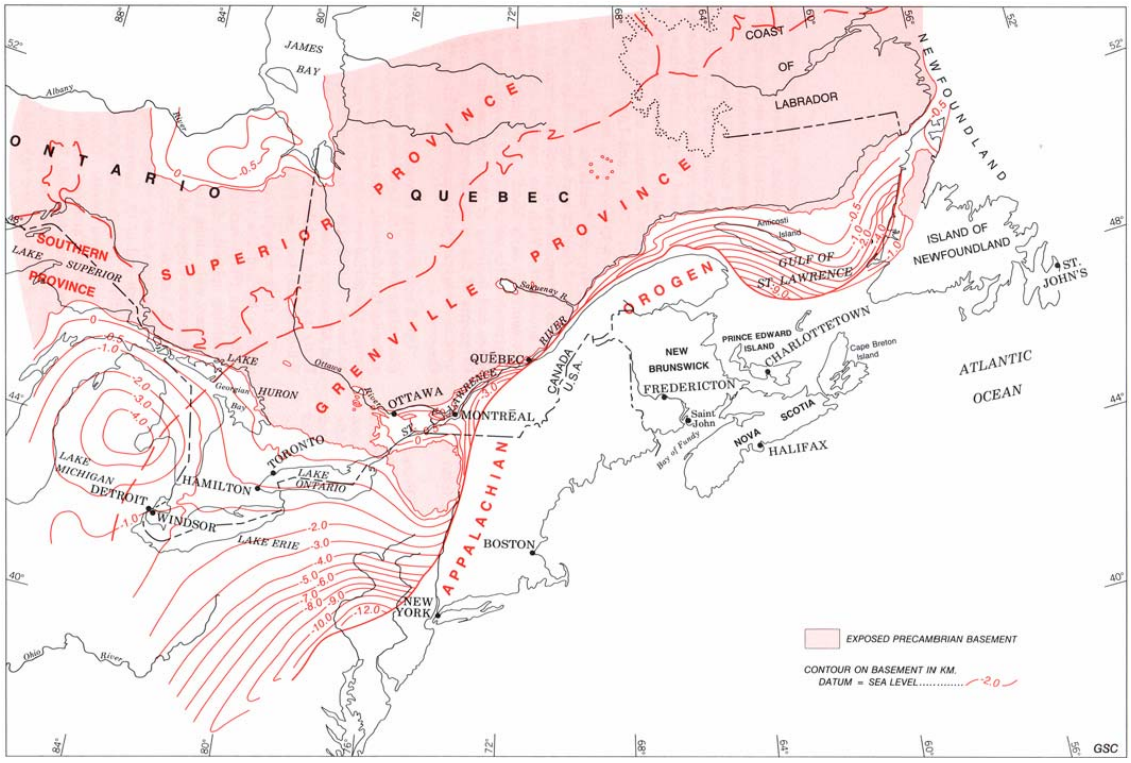

Figure 2.2. Configuration of Precambrian Basement Rocks Beneath Phanerozoic Cover, St. Lawrence Platform (after Sandford 1993b).

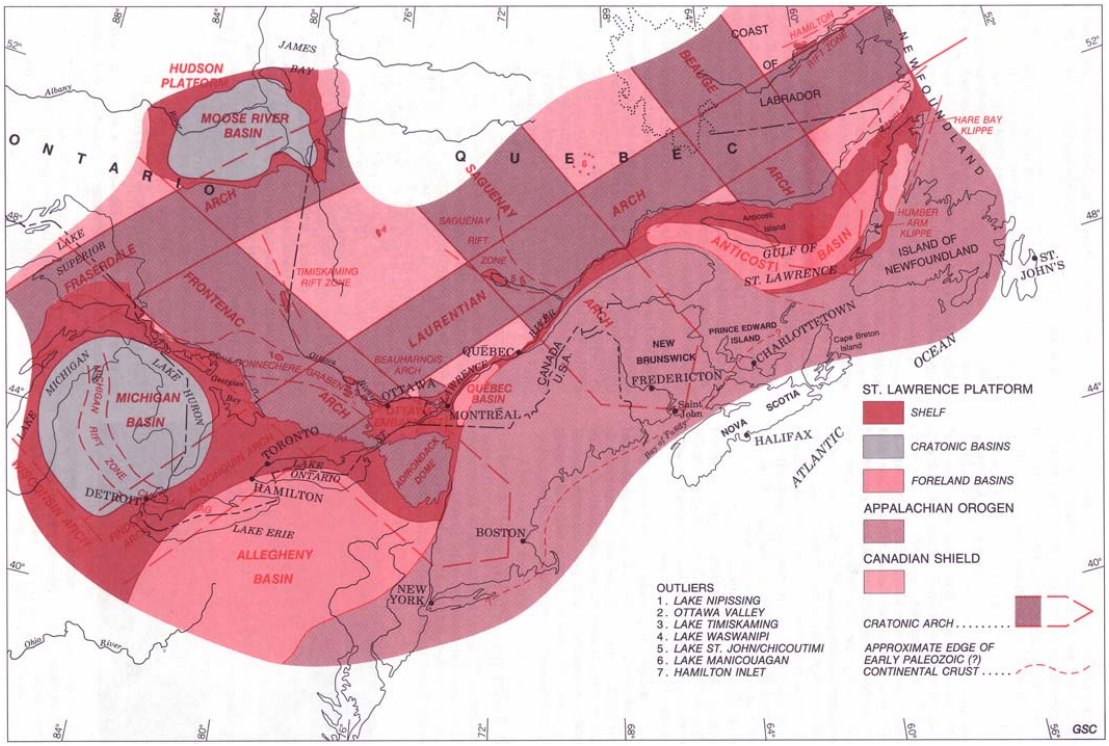

Figure 2.3. Principle Tectonic Elements of the St Lawrence Platform (after Sandford 1993b).

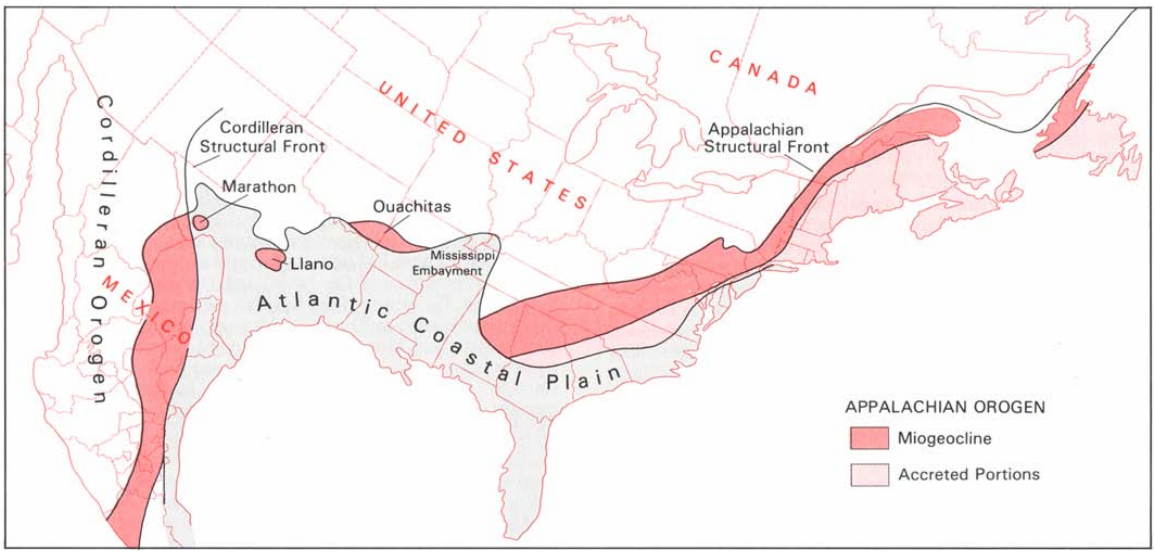

Figure 2.4. Appalachian Orogen, Newfoundland to Mexico (adapted from Williams 1995a).

Cooper et al. (2001) produced a palinspastic cross-section of the Humber zone Paleozoic sediments and described their depositional environments within the context of a tectonically evolving, eastern Laurentian continental margin. They grouped the Paleozoic strata of the Humber zone into six tectono-stratigraphic megasequences, which represent one Wilson Cycle (Figure 2.5). From oldest to youngest, these magasequences are as follows:

1. Synrift Megasequence (SRMS), (Late Proterozoic - Early Cambrian) deposited as eastern Laurentia began to rift apart to form the Iapetus (proto-Atlantic) ocean. These rocks comprise the lower part of the Labrador Group, and they were deposited as arkosic beds of the Bradore Formation and overlying limestones of the Forteau Formation.

2. Passive Margin Megasequence (PMMS), (latest Early Cambrian - Early Ordovician) that records shallow water carbonate sedimentation on the shelf passing eastward into basinal shales. This is analogous to the passive margin of eastern North America, particularly along its southern parts where carbonate sedimentation predominates.[1] In western Newfoundland, the shelf carbonates of this sequence contain the Watt's Bight and the Aquathuna formations, which are recognized reservoir rocks for hydrocarbons which are believed to originate from the hydrogen rich basinal shales of the Green Point formation. At its base this megasequence records progressive upward-deepening sedimentation from shallow marine reefal limestones into deeper marine shales of the Forteau Formation, which reflects thermal subsidence of the platform following cessation of active rifting (Williams and Hiscock 1987). Included in this megasequence are basinal shales of the Cooks Brook and Middle Arm formations, which were later thrust westward at least 100 km from their site of deposition by Taconic compression. These make up part of the Humber Arm allocthon.

[1] A "passive" margin is one where the transition from continental to oceanic crust is not characterized by the movement of one tectonic plate against another producing seismic activity, as is the case around the Pacific Ocean.

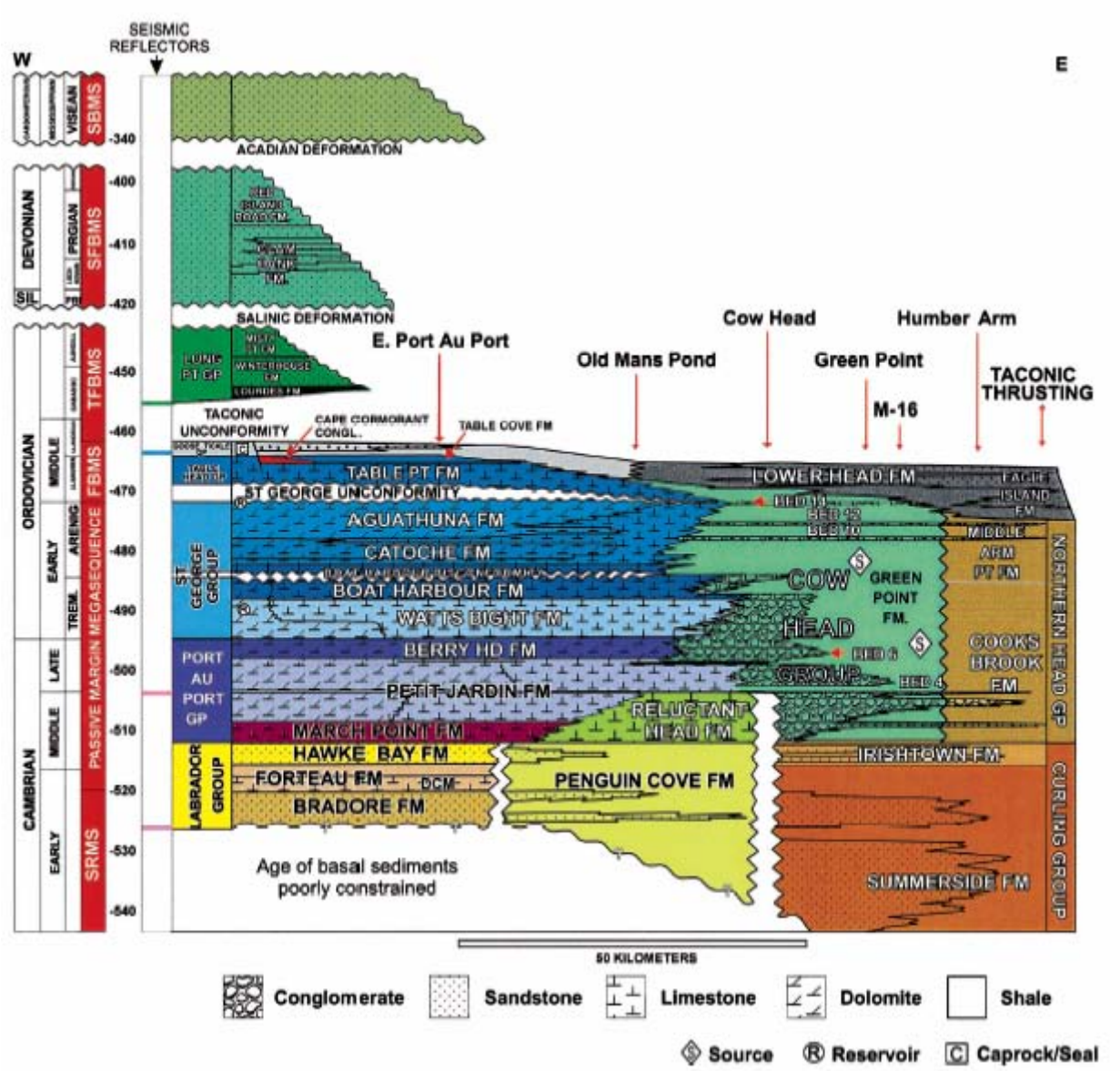

Figure 2.5. Palinspastic Reconstruction of Western Newfoundland Paleozoic Strata (adapted from Cooper et al. 2001)

Lithostratigraphic units are colored, and the ornamentation indicates the dominant lithology. The age ranges of the megasequences defined are shown to the right of the geological stages; SRMS = synrift megasequence; FBMS = flexural bulge megasequence; TFBMS = Taconic foreland basin megasequence; SFBMS = Salinic foreland basin megasequence; SBMS = successor basin megasequence.

3. Flexural Bulge Megasequence (FBMS), (Early to Middle Ordovician). The end of the stable platform and base of this megasequence is marked by the St George unconformity, which represents a depositional hiatus of three to four million years on the Port au Port Peninsula. This unconformity is recognized from Greenland to Quebec. The subsequent collapse of the

platform by extensional faulting is believed to have resulted from westward migration of the Taconic peripheral bulge (Knight et al. 1991). Sediments of the Table Head Group represent progressive deepening from shallow to deep subtidal limestones. The continued westward advance of the Taconic orogenic belt enhanced extensional block fault collapse of the platform. The Table Head Group and its distal correlatives the Cow Head Group are overlain by flysch of the Goose Tickle Group and Lower Head Formation, respectively, which marks a major reversal in sediment provenance from the east (interior carton) to the west (Taconic bulge).

4. Taconic Foreland Basin Megasequence (TFBMS), (Middle Ordovician). Culmination of the Taconic compression resulted in westward thrusting of basinal sediments (e.g., Humber Arm Allochthon) and Bay of Islands ophiolites[2] (likely originating from the Dunnage zone) over autochthonous shelf carbonates. Siliciclastic shallow marine sediments of the Long Point Group were deposited in the quiescent Taconic foreland basin during Late Ordovician to Salinic and onlapped the Taconic Allocthons[3]

5. Salinic Foreland Basin Megasequence (SFBM), (Silurian to Devonian). During the Salinic orogeny, a major unconformity, representing a time gap of 20 million years, was created that separates the TFBMS from this megasequence. Fluvial sands and shales of the Clam Bank Formation and terrestrial red beds of the Red Island Road Formation dominate the SFBM.

6. Successor Basin Megasequence (SBMS), (Carboniferous). This megasequence consists of the youngest preserved sediments in the Humber zone, which include fluvial sandstones, silts, shales, and local evaporites (salts, gypsum, etc) of the Anguille, Codroy, and Barachois Groups. Following the Acadian orogency, these Carboniferous sediments were deposited in the Bay St George and Deer Lake basins along the Cabot Fault, a zone of right lateral strike slip plate movement that developed these pull-apart basins.

2.1.2 Hydrocarbon Occurrence in the Study Area

The Paleozoic rocks of the Humber zone were the first in the Province to be recognized as having petroleum potential. In 1812, Mr. Parsons noticed oil floating on the surface of Parson's Pond on the Great Northern Peninsula, and in subsequent years numerous oil and gas seeps, bituminous residues, and oil shales were found in other areas. In 1867, Newfoundland's first oil well was drilled, and during the next 98 years up to sixty shallow wells were advanced in four areas (Parson's Pond, St. Paul's Inlet, Deer Lake Basin, and at Shoal Point on the Port au Port Peninsula), more than half of which encountered hydrocarbons. These wells were drilled with little knowledge of the geology, poor quality equipment, insufficient financing, and to depths that typically were less than 500 meters (it is now known that

[2] An ophiolite is a portion of the upper mantle and overlying oceanic crust that is emplaced onto continental crust during plate collision.

[3] Allocthon refers to a fault block that is transported from its original location by compressive tectonic forces along subhorizontal thrust faults. Autochthon refers to untransported rocks.

sediment thicknesses often exceed 3,000 meters in these areas). In 1965, the NALCO 65-I well was drilled at Parson's Pond to a depth of 1,302 meters. Until that time, this was the deepest well drilled in western Newfoundland, and it was advanced without the benefit of modern geophysical data. Nevertheless, it came very close to penetrating a major thrust slice that is now recognized from modern seismic information. Exploration efforts targeted either rocks in the area of surface oil seeps, or Lower Paleozoic strata of the Anticosti Basin.

A new era of oil exploration began in 1995 in western Newfoundland when Hunt Oil and its partner PanCanadian drilled the first modern well that was based on new seismic mapping and geological theory. This was the *Port au Port #1*, which encountered oil that was flow-tested at 2,000 bopd and 1.3 mmcf/d of gas from a carbonate reservoir at 3,400 metres depth. Data obtained from follow up drilling of four additional deep wells in the Port au Port area coupled with new geophysical data and interpretations have proven the presence of a viable petroleum system in deep Paleozoic rocks of western Newfoundland, as well as the presence of undrilled structures (NLDME 2000). Known hydrocarbon occurrences are shown on Figure 2.6.

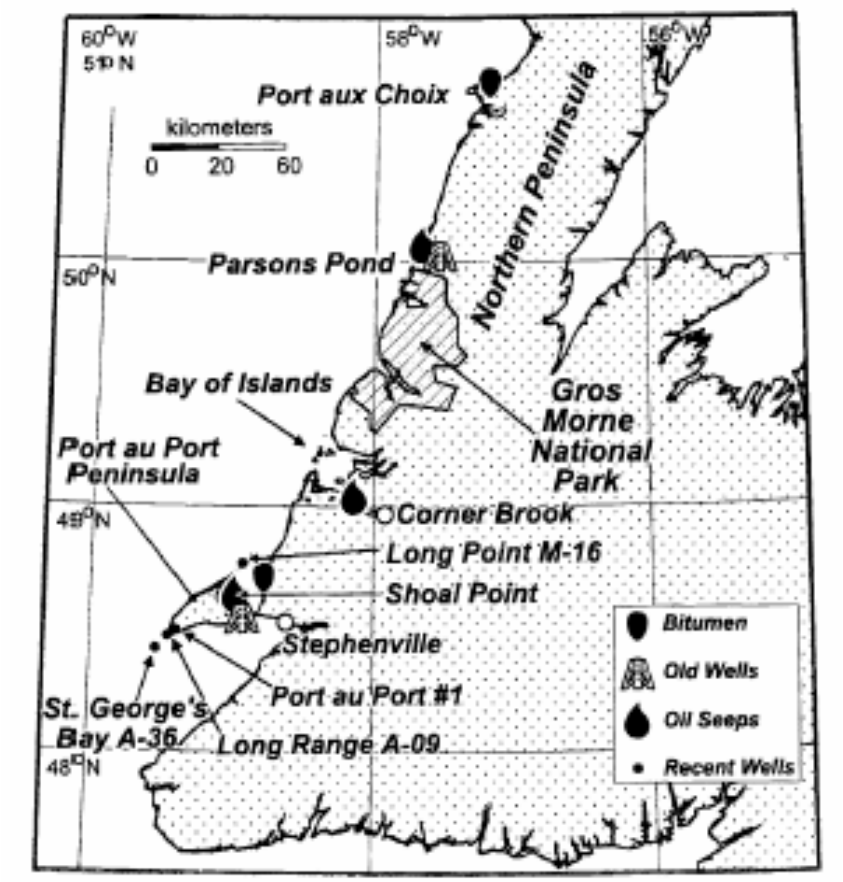

Figure 2.6. Location of Recent Wells, Older Wells, and Hydrocarbon Occurrences in the Humber Zone of Western Newfoundland (adapted from Cooper et al. 2001).

The current thinking on the region's hydrocarbon potential is provided by Cooper et al. (2001), and summarized by the Newfoundland and Labrador Department of Natural Resources (NLDME 2000). Sinclair (1990) provides a slightly dated but comprehensive overview of the hydrocarbon potential within the entire Study Area. The most current structural model of reservoir development associated with *Port au Port #1* in the Humber zone has the oil contained within Paleozoic carbonate rocks that have been subaerially exposed during the Middle Ordovician extensional faulting, followed by westward-directed compressional thrusting of allocthonous blocks during the Taconic orogeny, followed by porosity and permeability enhancement during the Devonian caused by dolomitizing hydrothermal fluids that migrated preferentially along old, reactivated fault zones, and finally by Acadian compression that created anticlinal reservoirs associated with footwall shortcut faults located below reactivated faults such as the Round Head Thrust fault, as shown on Figure 2.7. The model of reservoir formation is shown on Figure 2.8.

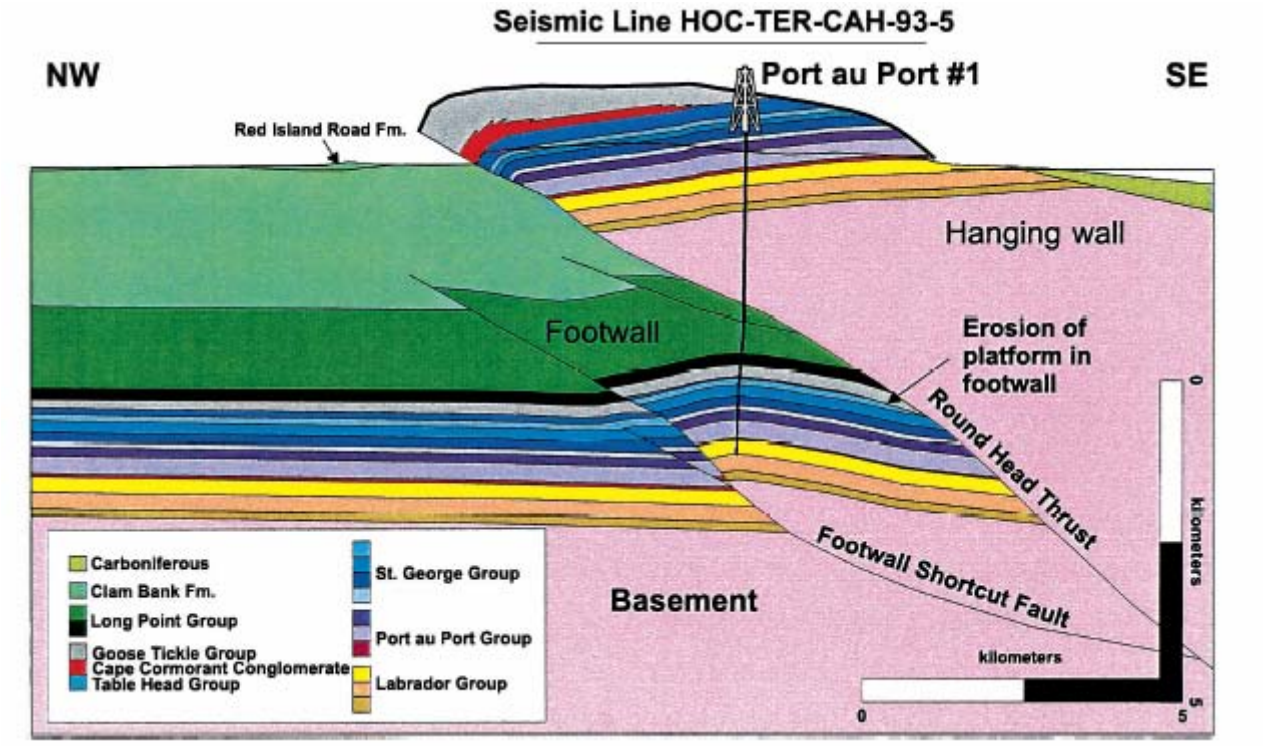

Figure 2.7. Structural Cross Section through *Port au Port #1* Well Based on Surface Geology, Seismic Data, and Dip and Formation Data from the Well (adapted from Cooper et al. 2001).

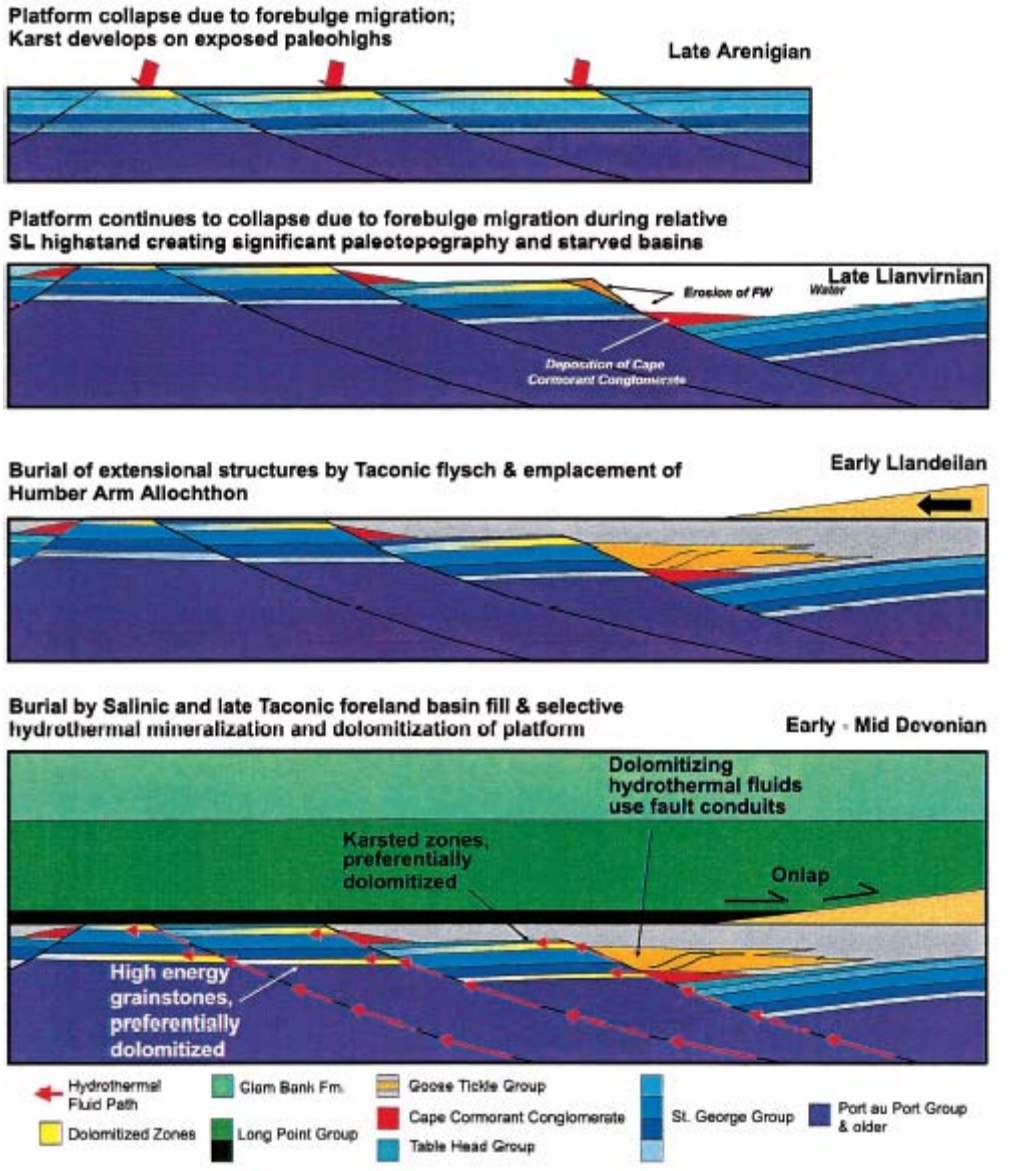

Figure 2.8. Model of Reservoir Development Based on Data from the Wells and Outcrop Studies (adapted from Cooper et al. 2001).

The area to the west of the Appalachian Structural Front within the undeformed Lower Paleozoic East St Lawrence Platform remains an untested area with good hydrocarbon prospects (Sinclair 1990).

2.1.3 Coastal Geomorphology

The coastline of the Study Area stretches from Cape Ray near Newfoundland's southwest corner to Reefs Harbour on the Great Northern Peninsula. The geomorphology of this area has been transformed by events of the past 14,000 years, associated primarily with the advance and retreat of the Laurentide and Newfoundland Ice Sheets and the influence of the sea on the land.

Glaciers scraped off large volumes of bedrock, crushed this into smaller boulders and to clay-sized particles, transported and deposited the resulting debris directly onto the hard surfaces (e.g., bedrock, land, seabed), or deposited it within and left it to be reworked by water. As the glaciers retreated the land rebounded in response to the release of tremendous pressures from the loss of ice and rock. This left areas that were once submerged beneath the sea now subaerially exposed. Evidence (embodied in radiocarbon dates and geomorphological records) has been found of ancient shorelines well above present sea levels throughout the west coast of Newfoundland. In fact, going from south to north along the west coast, historic maximum sea level stands can be found to progress from present sea levels near Cape Ray to about 140 m above sea level at the Strait of Belle Isle (Batterson et al. 2001).

"Type B" relative sea level curves (characterized by sea level falling from a recorded high stand following deglaciation to below the present level, and subsequently rising again) are typical for most of the island. This is the case for much of the southern part of the Study Area, but "Type A" curves (with sea level falling continuously from a high marine limit to present levels) are more representative of the coastline north of Port au Choix (Liverman 1994).

The following description of the coastal geomorphology of the west coast progresses from south to north along the eastern part of the Study Area.

Much of the southern section, from Cape Anguille to Highlands consists of a 50 km linear coastline dominated by cliffs of the Anguille Mountains that rise directly out of the sea. This stretch of coastline has relatively few, small pocket beaches.

Extending from Highlands at the foot of the Anguille Mountains to Romaines, west of Stephenville is the area of St George's Bay. This area has extensive exposures of unconsolidated sediments, deposited during the Late Wisconsinan glaciation and deglaciation. This stretch of shoreline has the thickest and most continuous surficial cover of any region in Newfoundland (Batterson et al. 2001). It is dominated by glacial marine, glaciomarine, marine sediments, and diamicton along elevated coastal bluffs and raised deltas that are up to 75 m above present sea level. In the northern part, around Flat Bay and Port Harmon, coastal sediments derived from erosion of proglacial deposits have accumulated to form large strand plains and beaches.

The area around Port au Port Peninsula starting and ending at its isthmus near Romaines is characterized by raised terraces, paleocliffs, raised marine deltas, and beaches. The southern part of Port au Port Bay is separated (West Bay and East Bay) by a prominent, bedrock cored point of land (Shoal Point). These are relatively flat, saltwater marshes that record a modern rising sea level.

The coastline from Port au Port isthmus to Fox Island River is characterized by a broad coastal plain with well-developed beach systems and barrier bars. The community of Fox Island River is built on a large raised delta at the mouth of Fox Island River. Sea level in this area fell rapidly from its highstand of 45 m above sea level about 13,500 years ago and crossed the modern datum about 12,200 years ago, falling to a lowstand of -25 m above sea level, and has been steadily rising ever since.

To the north, from Fox Island River to Rocky Harbour, the coastline is generally dominated by steep bedrock cliffs of the Long Range Mountains. This stretch includes the Bay of Islands and Bonne Bay. A massive rock slide into Bonne Bay involving about 10 billion m^3 of volcanic and metamorphic rock occurred in post glacial times. The fault scarp can be traced for several kilometres on the west side of Bonne Bay, about 0.5 km north of Woody Point. In general, poor road access for much of this area has restricted geomorphological investigation of most of this area in comparison with other parts of the Study Area coastline. However, the Geological Survey of Canada (Atlantic Region) has recorded much of the coastline with video footage that is available (J. Shaw, pers. comm.).

The coastline north from Rocky Harbor to Parsons Pond is marked by a linear shoreline with flat features such as an intertidal rock platform at Green Point, and coastal lowlands and lake basins such at Western Brook Pond, Parsons Pond, St Paul's Inlet, Bakers Brook Pond, and Ten Mile Pond. These areas are underlain by a thick blanket of soft, stony, sub-stratified shell bearing sediments interpreted to be submarine till laid down beneath floating ice shelves (Grant 1987). Beaches along the shoreline with sand dunes, such as at Western Brook Pond, are common.

The coastline from Parsons Pond to Hawkes Bay is linear, generally with sediment bluffs overlying bedrock typically exposed along long, linear beach systems. The bluffs are typically less thick than those along the Port au Port and St George's Bay coastline.

The coastline from Hawkes Bay to northern limit of the Study Area is characterized by headlands and deep bays, again with relatively thin sediment layers over bedrock, both of which are exposed along the shoreline in long beach systems.

2.1.4 Seismicity of the Offshore Western Newfoundland Study Area

The potential for damage to a structure by an earthquake is primarily determined by two things: the nature of associated ground movements at the site of a structure, and the construction elements of the structure itself. In Canada, expected ground motions (also referred to as "seismic hazard") are calculated on the basis of probabilistic theory and are represented by seismic zoning maps, as shown in Figures 2.9 and 2.10 (NRCan website 2005)

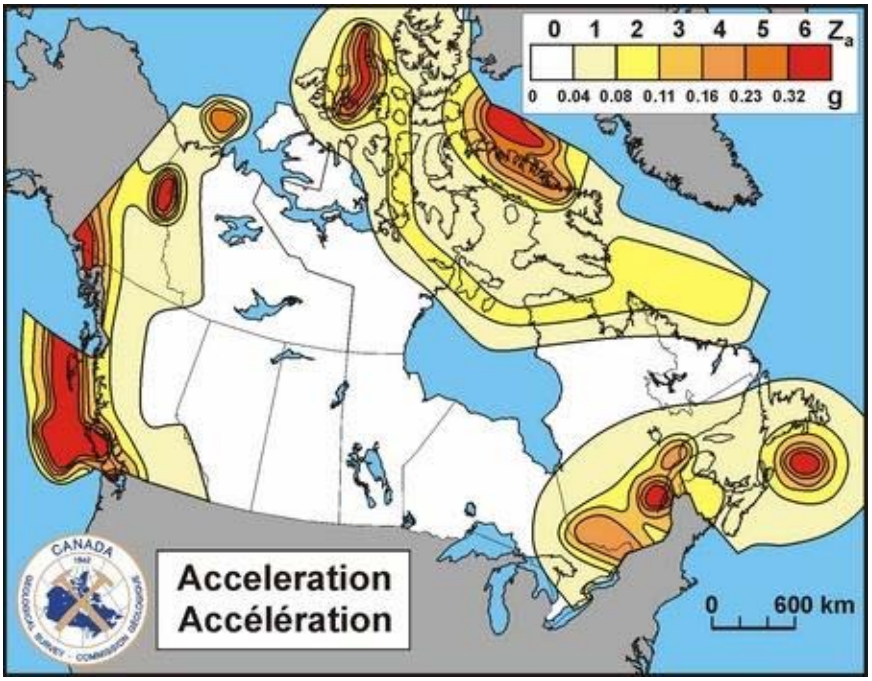

Source: NRCan Website 2005.

Figure 2.9. Seismic Zoning Map of Canada, 1985: Peak Horizontal Ground Acceleration (g) (Probability of Exceedance: 10% in 50 Years).

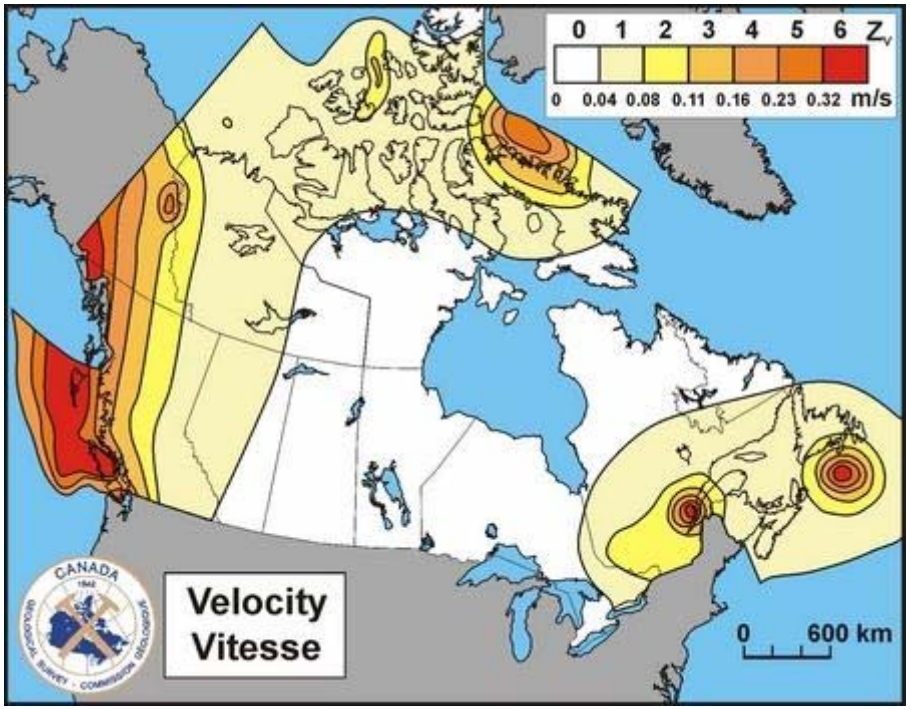

Source: NRCan Website 2005.

Figure 2.10. Seismic Zoning Map of Canada, 1985: Peak Horizontal Ground Velocity (m/s) (Probability of Exceedance: 10% in 50 Years).

These maps show peak horizontal ground accelerations and peak horizontal ground velocities, respectively. They have been prepared by the Geological Survey of Canada and are derived from statistical analysis of past earthquakes and from advancing knowledge of Canada's geology. Peak accelerations and velocities define seismic zones throughout Canada, that range from zero (which represent relatively aseismic areas of the Canadian Shield) to six (which represent areas that are the most seismically active within the country).

Although representation of regional seismic hazard has been developed for construction of land-based buildings as part of the National Building Code, the maps also provide an indication of relative seismic hazard for offshore structures, in particular those used for offshore oil exploration and production (Heidebrecht et al. 1983; Adams 1986; Anon. 1992).

The Study Area falls within Zone 1, and is therefore considered to have a relatively low seismic hazard with respect to peak horizontal ground accelerations and velocities.

2.2 Bathymetry

Water depths within the SEA Study Area range from intertidal to >500 m (see Figure 1.1). Approximately 70% of the Study Area is continental shelf (<200 m) and the remainder is slope (200 to >500 m depths). Detailed bathymetry is shown in Figure 1.1.

2.3 Climatology

The weather of the Study Area is governed by the transit of low and high-pressure systems. These circulation systems are embedded in the prevailing westerly flow that typifies the upper levels of the atmosphere in the mid-latitudes as caused by the normal tropical to polar temperature gradient. The mean strength of the westerly flow is a function of the intensity of this gradient, and as a consequence, it is considerably stronger in the winter months when there is a greater increase in the south to north temperature gradient than during the summer months.

When the upper level long wave trough lies well west of the region, the main storm track lies through the Gulf of St. Lawrence. Under this regime, an east to southeast flow ahead of a warm front associated with a low will give way to winds from the south in the warm sector of the system. Typically, the periods of southerly winds and mild conditions have relatively long durations and, in general, the incidence of extended storm conditions is likely to be relatively infrequent. Strong frictional effects in the stable flow from the south results in a marked shear in the surface boundary layer and relatively lower winds at the sea surface. As a consequence, local wind wave development tends to be inhibited under such conditions. Precipitation types are more likely to be in the form of rain or drizzle, with relatively infrequent periods of continuous snow. Periods of snow showers will prevail in the unstable air in the wake of cold fronts associated with the lows. Visibility will be reduced at times in frontal and advection fogs, in snow, and during snow shower activity.

At times when the upper long wave trough is to the east, the main storm track may lie through or to the east of Newfoundland. With the lows passing to the east of the Gulf of St. Lawrence, and frequent high potential for storm development, the incidence of strong gales is high. During long bouts of cold, west to northwest winds behind cold fronts occur frequently, and because the flow is colder than the surface water temperatures, the surface layer is unstable. The shear in the boundary layer is low, resulting in relatively high wind speeds near the surface and, consequently, relatively high sea state conditions. When very low air and sea surface temperatures are coupled with high winds, the potential for freezing spray occurs quite frequently until the area freezes over. In this synoptic situation, a greater incidence of precipitation in the form of snow is likely to occur. Freezing precipitation, either as rain or drizzle, may occur relatively often over the Port au Port area. Visibility will be reduced in frontal and advection fogs and by snow.

In winter, the Port au Port area is affected by cold arctic air which pours off the Quebec North Shore and crosses the relatively warm waters of the Gulf of St. Lawrence (prior to the formation of ice). The cold air picks up heat and moisture from the waters below resulting in the development of streamers of snow showers that hit the west coast of Newfoundland. For example, Stephenville Airport (48° 32′N; 58° 33′W) receives, on average, more than four metres of snow per year.

Intense low-pressure systems frequently become ‘captured’ and either slow down or stall under an upper air low-pressure centre as they move through the Newfoundland region or across the Labrador Sea. This may result in an extended period of little change in weather conditions that may range, depending on the position, overall intensity and size of the system, from relatively benign to heavy weather conditions.

By summer, the main storm tracks have moved further north than in winter, typically resulting in less frequent and weaker low-pressure systems. With increasing solar radiation during spring, there is a general warming of the atmosphere that is relatively greater at high than low latitudes. This decreases the north-south temperature contrast, lowers the kinetic energy of the westerly flow aloft, and decreases the potential energy available for storm development. Concurrently, there is a northward shift of the main band of westerly winds at upper levels and a marked development of the Bermuda-Azores sub-tropical high-pressure area to the south. This warm-core high-pressure cell extends from the surface through the entire troposphere. The main track of the weaker low-pressure systems typically lies through the Labrador region and tends to be oriented from the west-southwest to the east-northeast.

With low pressure systems normally passing to the north of the region in combination with the northwest shoulder of the sub-tropical high to the south, the prevailing flow across the Gulf of St. Lawrence is from the south to southwest during the summer season. Wind speed is lower during the summer and the incidence of gale or storm force winds relatively low. There is also a corresponding decrease in significant wave height.

The prevailing south to southwesterly flow during the late spring and early summer tends to be moist and relatively warmer than the underlying surface waters of the Gulf of St. Lawrence. Cooling from below coupled with mixing of the air in the near-surface layer frequently results in saturation of the air,

the condensation of water vapour, and the development of advection fog, which can persist for days at a time. The incidence of advection fog and the frequency of poor visibility are normally highest during July.

2.3.1 Wind Conditions

This section is based on the AES-40 data set (see Swail et al. 1999; Swail and Cox 2000) that contains 49 years (1954-2003) of climatology data for a number of points in the Gulf of St. Lawrence. Grid point 5817 (48.75°N; 59.17°W) was deemed to be the most representative for this study (Figure 2.11). Winds are 10 m above the surface and considered to be 1-hour mean values.

The percentage of observations of wind speed by direction is shown in Table 2.1. Directions are binned in 45º intervals centred on the directions shown. The table shows that the winds occurred most often from the west to northwest from November to March. In April, winds most often occurred from the southwest to northwest. South to southwest winds dominated from May to August. Southwest to west winds were predominant in September and October.

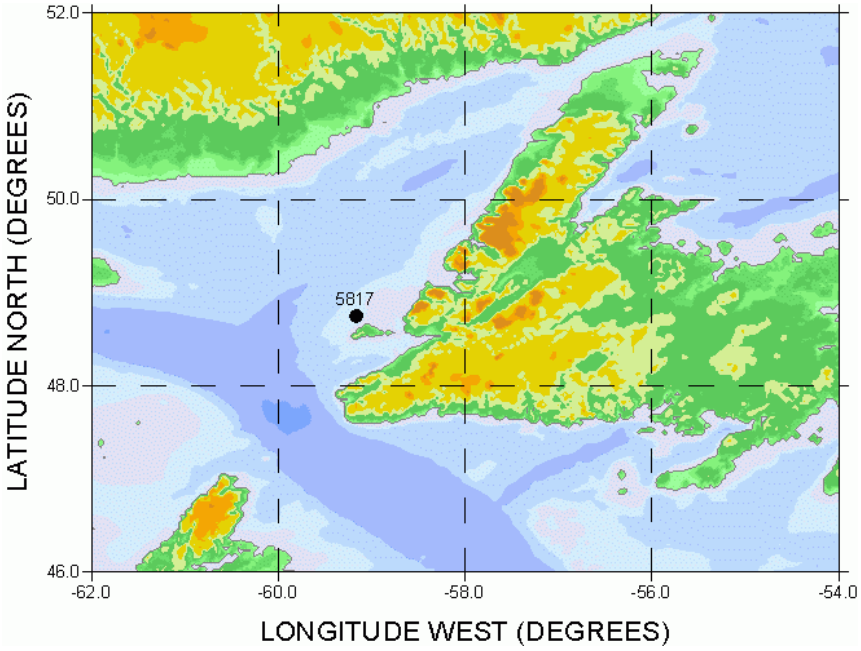

Figure 2.11. Location of Grid Point 5817.

Table 2.1. Percentage of Wind by Direction for AES Grid Point 5817.

Month	Direction								Total
	NE	E	SE	S	SW	W	NW	N	Reports
January	8.1	6.1	5.8	8.4	14.2	25.5	21.9	10.1	6076
February	8.8	6.4	6.2	8.4	14.0	23.3	20.7	12.2	5536
March	12.6	7.5	7.0	10.4	13.9	16.7	17.3	14.6	6076
April	12.4	9.8	10.5	11.4	13.9	13.4	14.0	14.6	5880
May	10.3	9.1	9.4	18.7	18.9	11.9	10.8	10.8	6076
June	6.5	6.4	8.8	22.5	26.6	12.7	8.9	7.5	5880
July	2.8	4.1	7.6	26.3	33.2	15.2	6.6	4.2	6076
August	4.6	4.7	6.0	19.1	32.9	18.2	8.5	5.9	6076
September	5.5	5.0	5.9	15.6	24.9	22.4	12.8	7.9	5880
October	5.7	4.6	7.1	13.0	20.4	21.6	17.1	10.5	6076
November	7.2	6.4	6.9	12.1	16.4	21.9	19.7	9.6	5880
December	6.7	5.7	6.5	9.3	13.5	23.6	22.0	12.6	6076
Years Mean	7.6	6.3	7.3	14.6	20.2	18.9	15.0	10.0	

Source: AES grid point 5817. Lat 48.75°N, Long 59.17 °W, 1954 to 2003.

Table 2.2 shows the highest winds (maximum 1-hour sustained winds) that occur by month in each of eight directions. The highest wind of 25 m/sec occurred in December and January. In January, the highest winds were from the northwest to north whereas in December the highest winds were from the southwest. The lowest maximum winds were in July. [To convert 1-hour means to 1-minute means (gusts), multiply by 1.18—UK Dept. of Energy 1984.]

Table 2.2. Monthly Highest 10 Metre Wind Speed (rounded to the nearest m/s) from each Direction at Grid Point 5817.

Month	Direction								Monthly	
	NE	E	SE	S	SW	W	NW	N	Min	Max
January	23	24	21	23	21	21	25	25	21	25
February	24	20	21	20	20	21	22	20	20	24
March	20	23	19	18	18	24	23	21	18	24
April	19	19	17	16	17	18	18	21	16	21
May	16	19	14	19	19	19	16	15	14	19
June	17	13	13	14	14	14	14	15	13	17
July	14	10	15	15	14	13	13	15	10	15
August	14	14	17	15	14	16	13	16	13	17
September	15	21	15	18	19	18	19	18	15	21
October	21	20	19	20	17	21	19	19	17	21
November	18	20	22	22	20	22	21	21	18	22
December	20	18	22	22	25	22	22	24	18	25
Years Max	24	24	22	23	25	24	25	25		

Source: AES grid point 5817. Lat 48.75°N, Long 59.17°W, 1954 to 2003.

Table 2.3 gives the monthly mean wind speed, standard deviation and maximum wind speeds. Gale force winds (17.2 to 24.4 m/s) occurred in all months except July and August. Storm force winds (24.5 to 32.6 m/s) occurred in January and December. Hurricane force winds (greater or equal to 32.7 m/s) did not occur at the grid point.

Table 2.3. Monthly Statistics; Mean Wind Speed, Standard Deviation, Maximum Wind Speed (m/s) for Grid Point 5817.

Month	Mean Speed	Standard Deviation	Maximum Speed
January	9.15	3.65	25.01
February	7.5	3.55	23.58
March	7.23	3.52	23.59
April	6.64	3.26	21.42
May	5.44	2.86	19.03
June	5.07	2.6	17.35
July	4.96	2.39	14.76
August	5.49	2.47	16.72
September	6.7	2.97	20.86
October	7.81	3.12	21.47
November	8.63	3.41	22.37
December	9.32	3.7	25.01

Source: AES grid point 5817. Lat 48.75°N, Long 59.17°W, 1954 to 2003.

Winter, spring, summer and fall winds roses for the grid point are plotted in Figures 2.12 to 2.15. The data for all months are provided in Tables 2.4 to 2.15. The dominant wind directions are from the northwest, west, southwest and south. There is a strong annual cycle in the wind direction. In winter, the winds are from west to northwest, whereas in summer the winds are from south to southwest. In the transition month of April, winds are distributed throughout all directions.

The bivariate histograms of the wind speeds versus directions in Tables 2.4 to 2.15 show that the wind speeds are much lower in summer than in winter. In general, November, December, and January are the months with the highest occurrence of higher wind speeds. High wind speeds can also occur in late summer and fall due to the passage of tropical systems but the frequency of high winds is lower.

The percentage exceedance of wind speeds at the grid point is shown in Figure 2.16. It should be noted that winds predicted from the AES40 data are representative of an areal average as well as an hourly average and that local winds may exceed these values. Site-specific EAs may examine coastal data from sources such as the Meteorolocal Services of Canada website: http://www.climate.weatheroffice.ec.gc.ca/Welcome_e.html.

Table 2.4. Percentages of Observations of Wind Speed by Direction for AES Grid Point 5817.

January

Wind Speed	Wind Direction (from)								
(m/s)	NE	E	SE	S	SW	W	NW	N	Total
0.00 - 4.99	1.05	1.09	1.05	1.20	1.70	1.96	2.39	1.42	11.85
5.00 - 9.99	4.76	2.85	2.81	4.25	7.19	12.21	11.24	5.25	50.56
10.00 - 14.99	1.88	1.71	1.40	2.29	4.59	9.08	6.96	2.80	30.71
15.00 - 19.99	0.39	0.33	0.44	0.64	0.61	1.94	1.32	0.58	6.25
20.00 - 24.99	0.07	0.05	0.05	0.02	0.02	0.12	0.15	0.13	0.59
25.00 - 29.99	0.00	0.00	0.00	0.00	0.00	0.00	0.02	0.02	0.03
30.00 - 34.99	0.00	0.00	0.00	0.00	0.00	0.00	0.00	0.00	0.00
Total	8.15	6.03	5.75	8.40	14.11	25.31	22.08	10.20	100.00
						Total Observations:			6076

Source: AES grid point 5817. Lat 48.75°N, Long 59.17°W, 1954 to 2003.

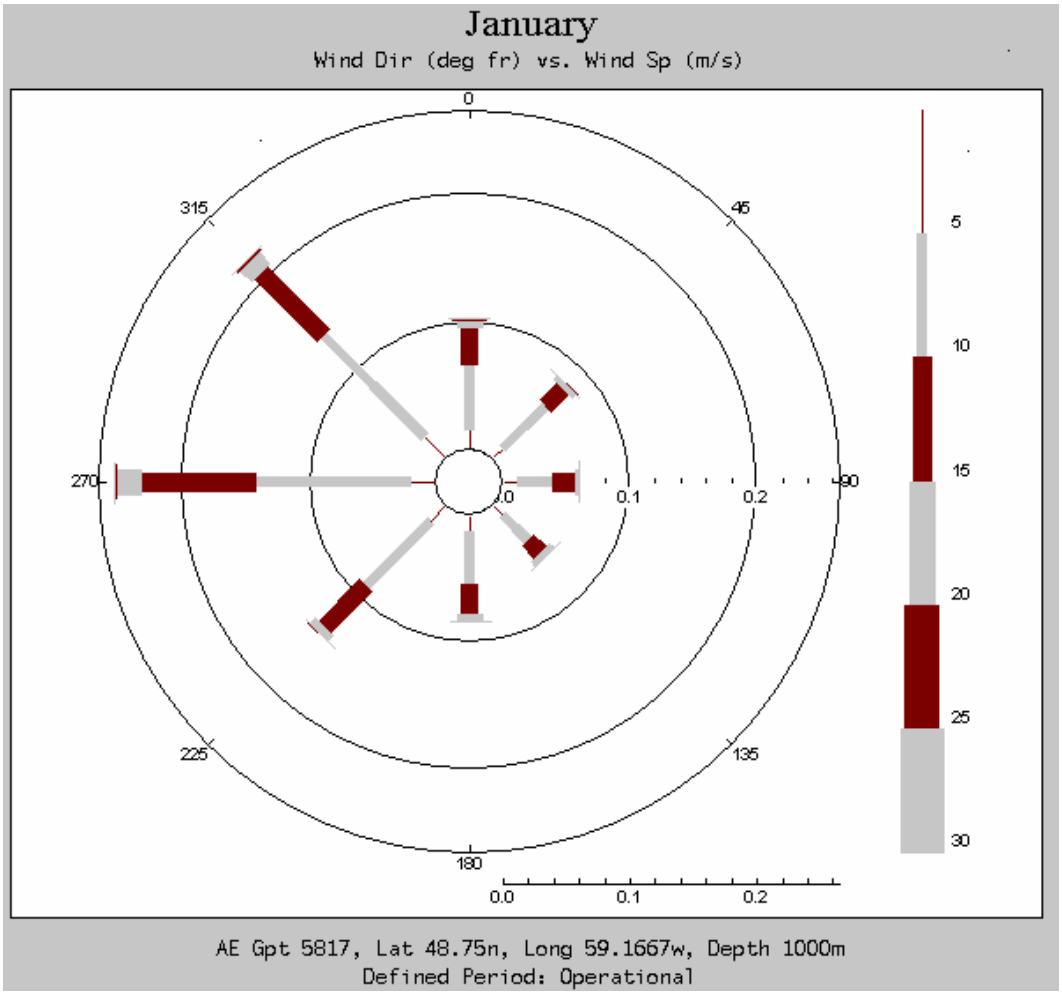

Figure 2.12. Wind Rose for January, Grid Point 5817.

Table 2.5. Percentages of Observations of Wind Speed by Direction for AES Grid Point 5817. February

Wind Speed	Wind Direction (from)								
(m/s)	NE	E	SE	S	SW	W	NW	N	Total
0.00 - 4.99	2.78	1.82	1.82	2.51	3.85	4.88	5.33	3.70	26.70
5.00 - 9.99	4.06	3.20	2.75	4.12	7.77	12.68	10.01	5.87	50.45
10.00 - 14.99	1.61	1.23	1.16	1.52	2.08	4.88	4.68	2.47	19.62
15.00 - 19.99	0.22	0.20	0.38	0.23	0.23	0.65	0.69	0.43	3.03
20.00 - 24.99	0.05	0.00	0.04	0.00	0.04	0.02	0.02	0.04	0.20
25.00 - 29.99	0.00	0.00	0.00	0.00	0.00	0.00	0.00	0.00	0.00
30.00 - 34.99	0.00	0.00	0.00	0.00	0.00	0.00	0.00	0.00	0.00
Total	8.72	6.45	6.15	8.38	13.97	23.11	20.73	12.51	100.00
						Total Observations:			5536

Source: AES grid point 5817. Lat 48.75°N, Long 59.17°W, 1954 to 2003.

Table 2.6. Percentages of Observations of Wind Speed by Direction for AES Grid Point 5817. March

Wind Speed	Wind Direction (from)								
(m/s)	NE	E	SE	S	SW	W	NW	N	Total
0.00 - 4.99	3.42	2.45	2.29	3.13	3.80	4.86	5.17	4.08	29.20
5.00 - 9.99	5.43	3.09	3.37	5.48	8.05	8.28	9.04	7.88	50.63
10.00 - 14.99	2.98	1.66	1.23	1.50	1.94	3.00	2.57	2.35	17.23
15.00 - 19.99	0.77	0.23	0.16	0.21	0.13	0.53	0.43	0.30	2.76
20.00 - 24.99	0.00	0.05	0.00	0.00	0.00	0.03	0.08	0.02	0.18
25.00 - 29.99	0.00	0.00	0.00	0.00	0.00	0.00	0.00	0.00	0.00
30.00 - 34.99	0.00	0.00	0.00	0.00	0.00	0.00	0.00	0.00	0.00
Total	12.60	7.48	7.05	10.32	13.92	16.70	17.29	14.63	100.00
						Total Observations:			6076

Source: AES grid point 5817. Lat 48.75°N, Long 59.17°W, 1954 to 2003.

Table 2.7. Percentages of Observations of Wind Speed by Direction for AES Grid Point 5817. April

Wind Speed	Wind Direction (from)								
(m/s)	NE	E	SE	S	SW	W	NW	N	Total
0.00 - 4.99	3.62	3.59	3.49	3.98	5.54	5.29	4.97	4.23	34.71
5.00 - 9.99	5.68	4.51	5.56	5.99	6.87	6.29	6.82	7.93	49.64
10.00 – 14.99	2.59	1.51	1.24	1.41	1.39	1.65	1.94	2.33	14.06
15.00 – 19.99	0.54	0.20	0.14	0.07	0.07	0.19	0.12	0.24	1.56
20.00 – 24.99	0.00	0.00	0.00	0.00	0.00	0.00	0.00	0.02	0.02
25.00 – 29.99	0.00	0.00	0.00	0.00	0.00	0.00	0.00	0.00	0.00
30.00 – 34.99	0.00	0.00	0.00	0.00	0.00	0.00	0.00	0.00	0.00
Total	12.43	9.81	10.43	11.45	13.87	13.42	13.85	14.74	100.00
						Total Observations:			5880

Source: AES grid point 5817. Lat 48.75°N, Long 59.17°W, 1954 to 2003.

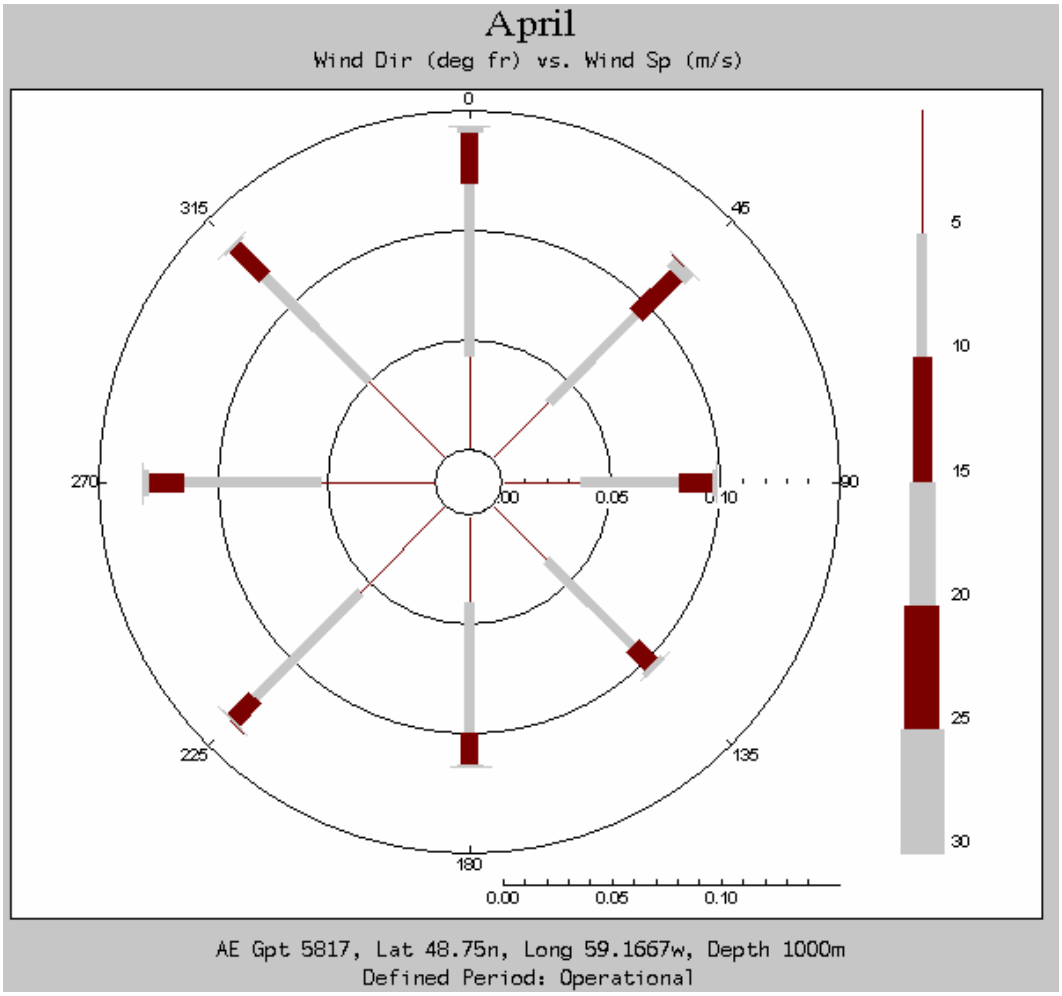

Figure 2.13. Wind Rose for April, Grid Point 5817.

Table 2.8. Percentages of Observations of Wind Speed by Direction for AES Grid Point 5817. May

Wind Speed	Wind Direction (from)								
(m/s)	NE	E	SE	S	SW	W	NW	N	Total
0.00 - 4.99	4.71	4.25	5.25	8.56	9.41	6.55	5.53	4.87	49.13
5.00 - 9.99	4.26	4.25	3.79	8.69	8.46	4.81	4.51	4.84	43.60
10.00 – 14.99	1.27	0.61	0.43	1.33	1.10	0.54	0.71	1.00	6.99
15.00 – 19.99	0.07	0.02	0.00	0.03	0.05	0.07	0.03	0.02	0.28
20.00 – 24.99	0.00	0.00	0.00	0.00	0.00	0.00	0.00	0.00	0.00
25.00 – 29.99	0.00	0.00	0.00	0.00	0.00	0.00	0.00	0.00	0.00
30.00 – 34.99	0.00	0.00	0.00	0.00	0.00	0.00	0.00	0.00	0.00
Total	10.31	9.13	9.47	18.61	19.02	11.97	10.78	10.73	100.00
						Total Observations:			6076

Source: AES grid point 5817. Lat 48.75°N, Long 59.17°W, 1954 to 2003.

Table 2.9. Percentages of Observations of Wind Speed by Direction for AES Grid Point 5817. June

Wind Speed	Wind Direction (from)								
(m/s)	NE	E	SE	S	SW	W	NW	N	Total
0.00 - 4.99	3.69	3.96	5.17	9.88	13.32	8.23	4.90	4.27	53.42
5.00 - 9.99	2.47	2.23	3.33	11.14	12.33	4.15	3.67	2.91	42.23
10.00 - 14.99	0.32	0.19	0.27	1.33	1.04	0.43	0.32	0.39	4.29
15.00 - 19.99	0.05	0.00	0.00	0.00	0.00	0.00	0.00	0.02	0.07
20.00 - 24.99	0.00	0.00	0.00	0.00	0.00	0.00	0.00	0.00	0.00
25.00 - 29.99	0.00	0.00	0.00	0.00	0.00	0.00	0.00	0.00	0.00
30.00 - 34.99	0.00	0.00	0.00	0.00	0.00	0.00	0.00	0.00	0.00
Total	6.53	6.38	8.77	22.35	26.69	12.81	8.89	7.59	100.00
						Total Observations:			5880

Source: AES grid point 5817. Lat 48.75°N, Long 59.17°W, 1954 to 2003.

Table 2.10. Percentages of Observations of Wind Speed by Direction for AES Grid Point 5817. July

Wind Speed	Wind Direction (from)								
(m/s)	NE	E	SE	S	SW	W	NW	N	Total
0.00 - 4.99	1.86	2.45	4.72	12.41	16.77	9.43	4.03	2.34	54.02
5.00 - 9.99	0.79	1.65	2.49	12.51	15.93	5.65	2.34	1.66	43.01
10.00 - 14.99	0.15	0.00	0.18	1.17	0.69	0.30	0.15	0.35	2.98
15.00 - 19.99	0.00	0.00	0.00	0.00	0.00	0.00	0.00	0.00	0.00
20.00 - 24.99	0.00	0.00	0.00	0.00	0.00	0.00	0.00	0.00	0.00
25.00 - 29.99	0.00	0.00	0.00	0.00	0.00	0.00	0.00	0.00	0.00
30.00 - 34.99	0.00	0.00	0.00	0.00	0.00	0.00	0.00	0.00	0.00
Total	2.80	4.10	7.39	26.09	33.39	15.38	6.52	4.34	100.00
						Total Observations:			6076

Source: AES grid point 5817. Lat 48.75°N, Long 59.17°W, 1954 to 2003.

Table 2.11. Percentages of Observations of Wind Speed by Direction for AES Grid Point 5817. August

Wind Speed	Wind Direction (from)								
(m/s)	NE	E	SE	S	SW	W	NW	N	Total
0.00 - 4.99	2.39	2.67	3.52	8.16	13.71	8.28	3.92	2.60	45.24
5.00 - 9.99	1.96	1.96	2.22	9.61	18.07	9.13	4.26	2.91	50.13
10.00 - 14.99	0.23	0.13	0.21	0.92	1.27	0.79	0.53	0.44	4.53
15.00 - 19.99	0.00	0.00	0.02	0.00	0.00	0.05	0.00	0.03	0.10
20.00 - 24.99	0.00	0.00	0.00	0.00	0.00	0.00	0.00	0.00	0.00
25.00 - 29.99	0.00	0.00	0.00	0.00	0.00	0.00	0.00	0.00	0.00
30.00 - 34.99	0.00	0.00	0.00	0.00	0.00	0.00	0.00	0.00	0.00
Total	4.58	4.76	5.97	18.69	33.05	18.25	8.71	5.99	100.00
						Total Observations:			6076

Source: AES grid point 5817. Lat 48.75°N, Long 59.17°W, 1954 to 2003.

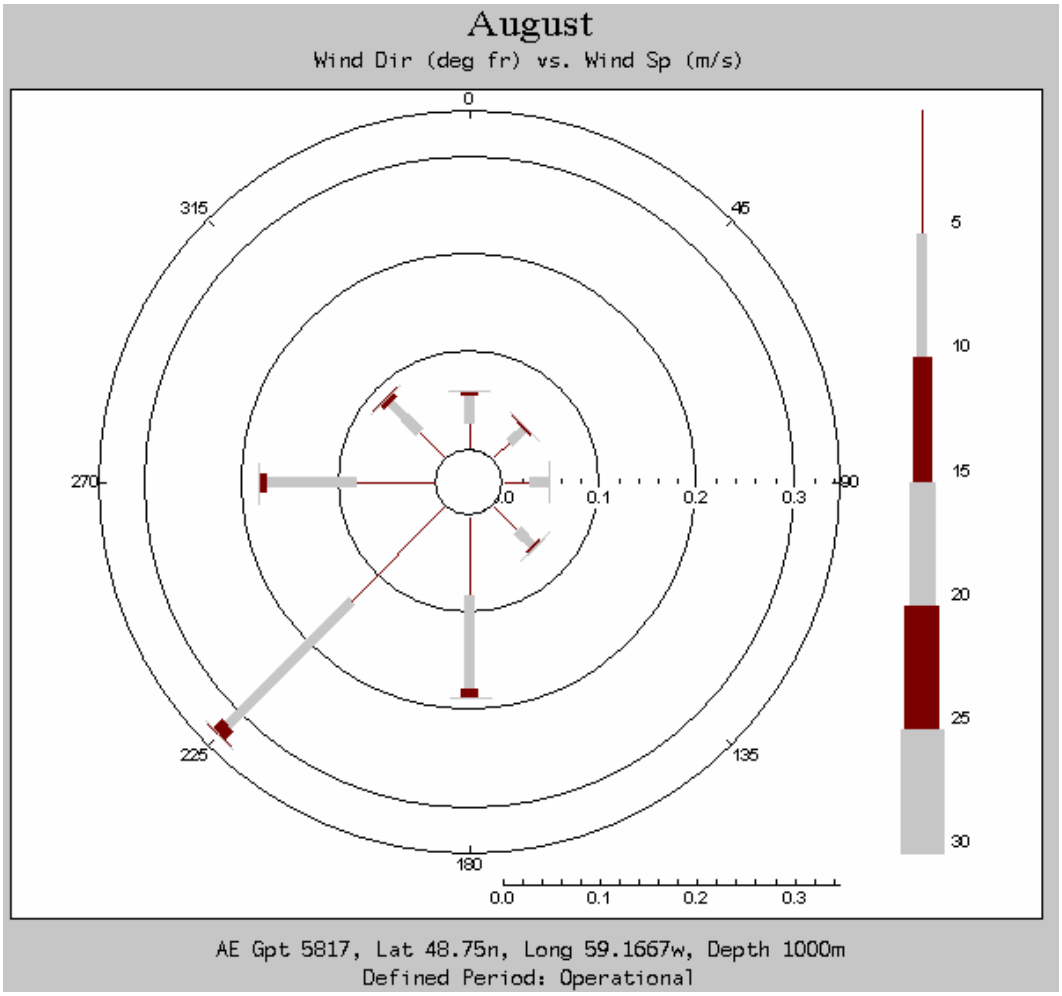

Figure 2.14. Wind Rose for August, Grid Point 5817.

Table 2.12. Percentages of Observations of Wind Speed by Direction for AES Grid Point 5817. September

Wind Speed	Wind Direction (from)								
(m/s)	NE	E	SE	S	SW	W	NW	N	Total
0.00 - 4.99	1.99	2.13	2.33	4.35	6.79	6.55	3.66	2.79	30.58
5.00 - 9.99	2.99	2.55	2.84	8.76	14.69	12.45	7.28	3.93	55.49
10.00 - 14.99	0.48	0.32	0.73	2.18	3.30	3.21	1.87	1.16	13.25
15.00 - 19.99	0.02	0.00	0.02	0.07	0.14	0.17	0.17	0.09	0.66
20.00 - 24.99	0.00	0.02	0.00	0.00	0.00	0.00	0.00	0.00	0.02
25.00 - 29.99	0.00	0.00	0.00	0.00	0.00	0.00	0.00	0.00	0.00
30.00 - 34.99	0.00	0.00	0.00	0.00	0.00	0.00	0.00	0.00	0.00
Total	5.48	5.02	5.92	15.36	24.92	22.38	12.98	7.96	100.00
						Total Observations:			5880

Source: AES grid point 5817. Lat 48.75°N, Long 59.17°W, 1954 to 2003.

Table 2.13. Percentages of Observations of Wind Speed by Direction for AES Grid Point 5817. October

Wind Speed	Wind Direction (from)								
(m/s)	NE	E	SE	S	SW	W	NW	N	Total
0.00 - 4.99	1.23	1.12	1.68	2.57	3.69	3.51	3.37	1.94	19.11
5.00 - 9.99	3.19	2.37	3.80	7.29	12.62	12.48	10.35	6.02	58.13
10.00 - 14.99	1.10	0.92	1.38	2.80	3.88	5.13	3.16	2.24	20.62
15.00 - 19.99	0.20	0.20	0.12	0.28	0.12	0.51	0.35	0.33	2.09
20.00 - 24.99	0.02	0.00	0.00	0.02	0.00	0.02	0.00	0.00	0.05
25.00 - 29.99	0.00	0.00	0.00	0.00	0.00	0.00	0.00	0.00	0.00
30.00 - 34.99	0.00	0.00	0.00	0.00	0.00	0.00	0.00	0.00	0.00
Total	5.74	4.61	6.98	12.96	20.31	21.65	17.23	10.53	100.00
						Total Observations:			6076

Source: AES grid point 5817. Lat 48.75°N, Long 59.17°W, 1954 to 2003.

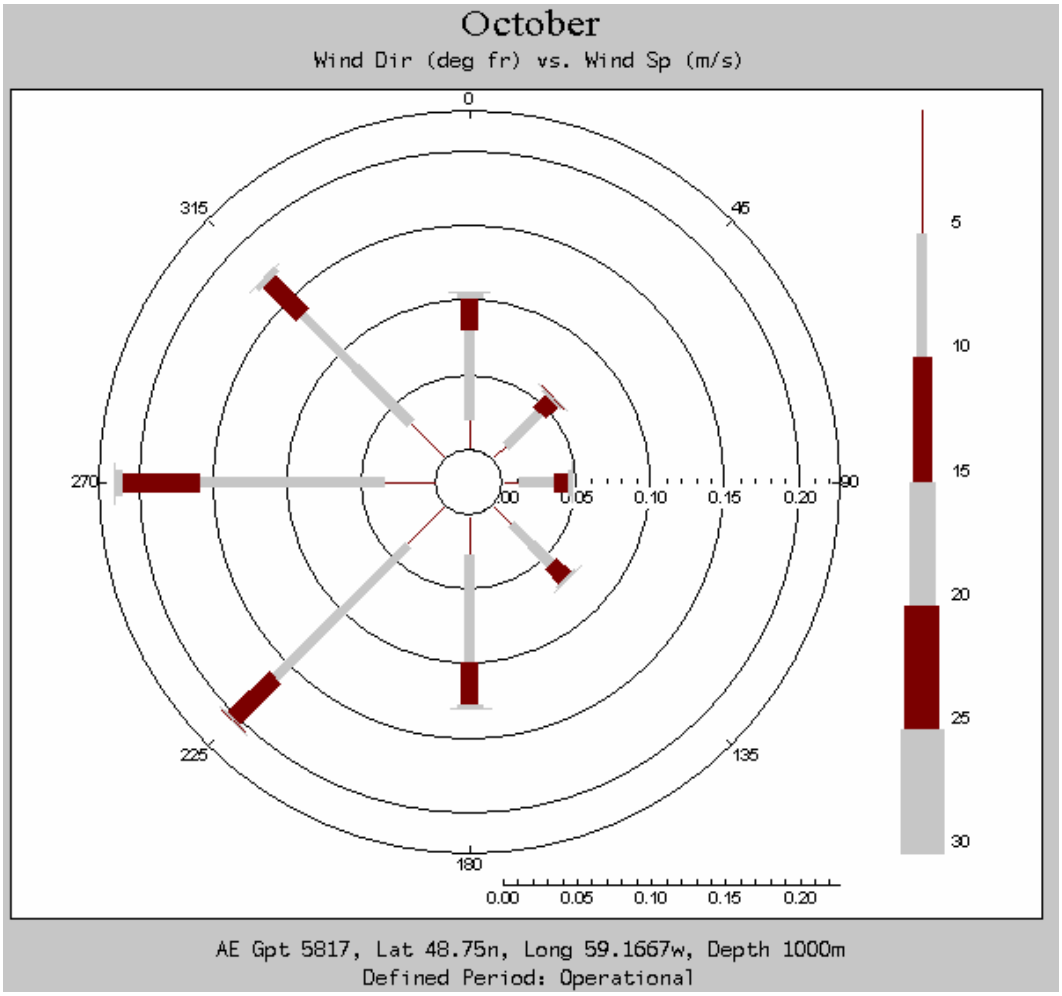

Figure 2.15. Wind Rose for October, Grid Point 5817.

Table 2.14. Percentages of Observations of Wind Speed by Direction for AES Grid Point 5817.

November

Wind Speed	Wind Direction (from)								
(m/s)	NE	E	SE	S	SW	W	NW	N	Total
0.00 - 4.99	1.09	1.09	1.39	1.87	2.47	2.60	2.60	1.48	14.59
5.00 - 9.99	3.95	3.91	3.30	6.12	9.47	11.34	10.36	5.12	53.57
10.00 - 14.99	1.84	1.28	1.89	3.33	4.08	6.65	5.63	2.41	27.11
15.00 - 19.99	0.24	0.17	0.27	0.61	0.37	1.16	1.11	0.66	4.59
20.00 - 24.99	0.00	0.00	0.02	0.02	0.00	0.05	0.03	0.02	0.14
25.00 - 29.99	0.00	0.00	0.00	0.00	0.00	0.00	0.00	0.00	0.00
30.00 - 34.99	0.00	0.00	0.00	0.00	0.00	0.00	0.00	0.00	0.00
Total	7.12	6.45	6.87	11.95	16.39	21.80	19.73	9.69	100.00
						Total Observations:			5880

Source: AES grid point 5817. Lat 48.75°N, Long 59.17°W, 1954 to 2003.

Table 2.15. Percentages of Observations of Wind Speed by Direction for AES Grid Point 5817. December

Wind Speed	Wind Direction (from)								
(m/s)	NE	E	SE	S	SW	W	NW	N	Total
0.00 - 4.99	1.28	0.91	0.84	1.40	1.53	1.79	2.17	1.73	11.65
5.00 - 9.99	3.23	2.63	3.04	4.38	7.49	11.21	10.60	6.44	49.01
10.00 - 14.99	1.91	1.79	1.76	3.00	3.79	8.15	7.27	4.08	31.75
15.00 - 19.99	0.28	0.30	0.77	0.61	0.63	2.14	1.84	0.51	7.08
20.00 - 24.99	0.03	0.00	0.02	0.02	0.10	0.12	0.13	0.08	0.49
25.00 - 29.99	0.00	0.00	0.00	0.00	0.02	0.00	0.00	0.00	0.02
30.00 - 34.99	0.00	0.00	0.00	0.00	0.00	0.00	0.00	0.00	0.00
Total	6.73	5.63	6.43	9.41	13.56	23.41	22.01	12.84	100.00
						Total Observations:			6076

Source: AES grid point 5817. Lat 48.75°N, Long 59.17°W, 1954 to 2003.

2.3.2 Weather

In this section, sea surface temperatures (SST) are derived from an analysis performed on NOAA-JPL's AVHRR weekly 18 km MCSST dataset, 1981 to 2000. The multichannel sea surface temperature (MCSST) product from NOAA's polar orbiting satellite is available from January of 1981 through January of 2001. This dataset is distributed at a spatial resolution of 18 km at weekly time periods. Error estimates for this dataset are approximately 0.5-0.7 Celsius degrees.

The air temperatures and visibility data were derived by simple interpolation from the Climatological Charts of the St. Lawrence (Environment Canada 1994). The charts incorporate all available land and ship observations to derive the frequency of visibilities of less than one kilometre. For air temperature, a

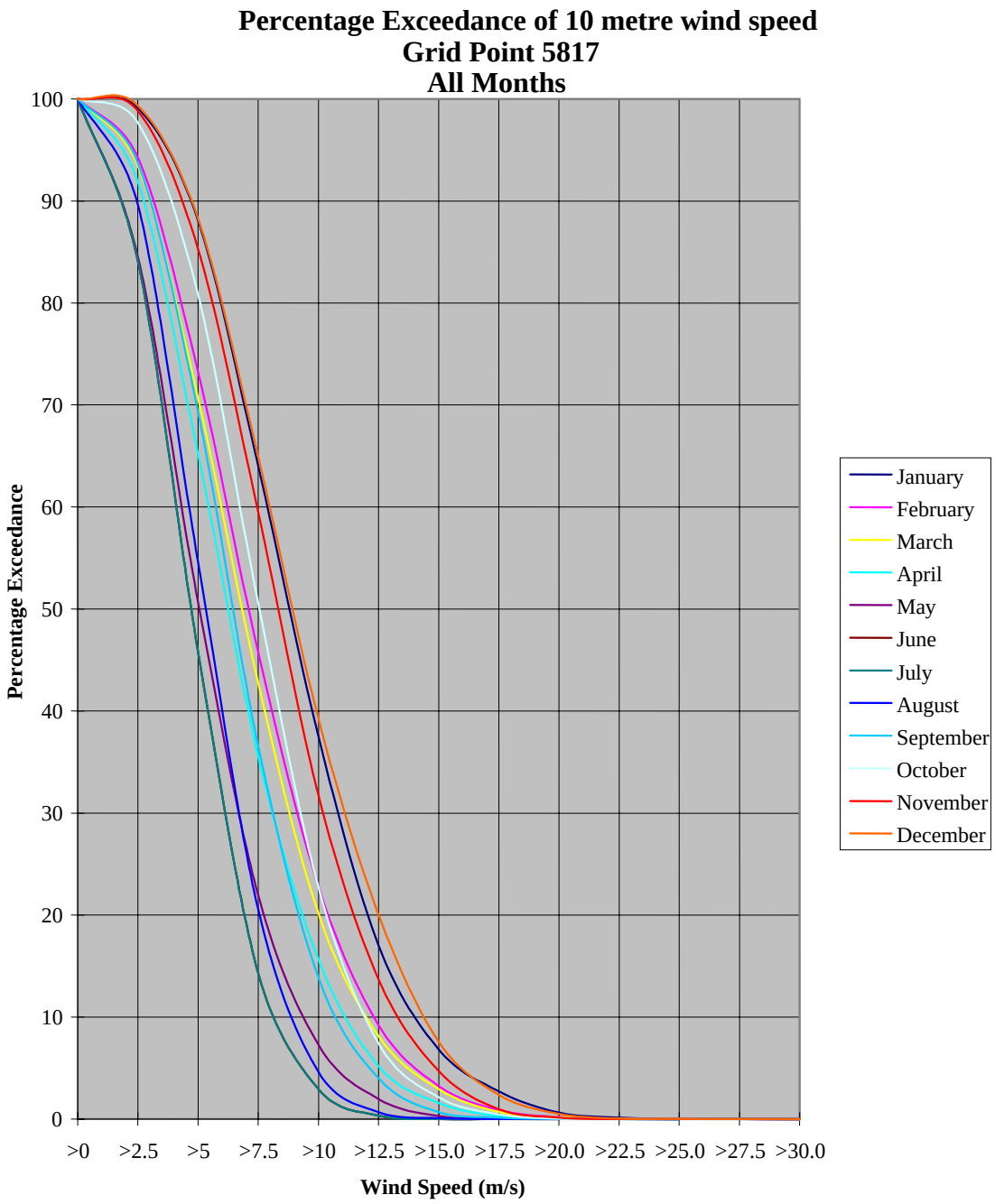

Source: AES grid point 5817 Lat 48.75°N, Long 59.17°W , 1954 to 2003.

Figure 2.16. Percentage Exceedance of 10 m Wind Speed at Grid Point 5817.

simple relationship was established between the air temperature at coastal stations and the temperature at sea according to the wind and water temperature. Two years of observations recorded by a weather buoy anchored off the coast of Mont Louis (49° 33′N 65° 45′W) provided these data at sea.

2.3.2.1 Air, Sea and Surface Temperatures

The air temperature follows a normal annual cycle with the minimum mean temperature in February of -6.5°C and the maximum mean temperature in August of 16°C (Figure 2.17).

The mean annual sea surface temperature cycle is also shown in Figure 2.17. The minimum mean temperatures are in February (-0.79 °C) and March (-0.75 °C). The maximum means are in August (15.32 °C) and September (15.52 °C).

2.3.3 Visibility

Figure 2.18 shows the percentage occurrence of visibilities less than one kilometre near grid point 5817. The relatively high occurrence in January, February and March tend to be due to reduced visibilities in snow. In April, as the snow turns to rain, the reduced visibilities tend to be the result of advection fog. Advection fog forms when warm moist air moves over the cooler waters of the Gulf. The air is cooled from below and becomes saturated, resulting in the formation of fog. Figure 2.17 indicates that the mean air temperature in April rises above the mean sea surface temperature. Advection fog subsequently increases during May, June and July. In August, the temperature difference between the air and the sea lessens and the occurrence of fog decreases. The air temperature falls below the sea surface temperature in September. October has the lowest occurrence of visibilities less than one kilometre because advection fog is minimal and the winter snow has yet to arrive.

2.3.4 Waves

The data source used here was the AES-40 hindcast data set for 49 years (1954-2003) generated by Oceanweather Inc. using their third generation deep-water wave model with input from the wind data previously described. The wave model grid spacing was 0.625º latitude by 0.833º longitude.

The main parameters that describe wave conditions are significant wave height, maximum wave height, spectral peak period, and characteristic period. The significant wave height is the average height of the 1/3 highest waves. Its value approximates the characteristic height observed visually. The maximum height is the greatest vertical distance between a wave crest and adjacent trough. The spectral peak period is the period of the waves with the largest energy levels, and the characteristic period is the period of the group of largest waves in a given sea state. It approximates the period of the 1/3 highest waves. The characteristic period is the wave period reported in ship observations, and the spectral peak period is reported in the AES-40 data set.

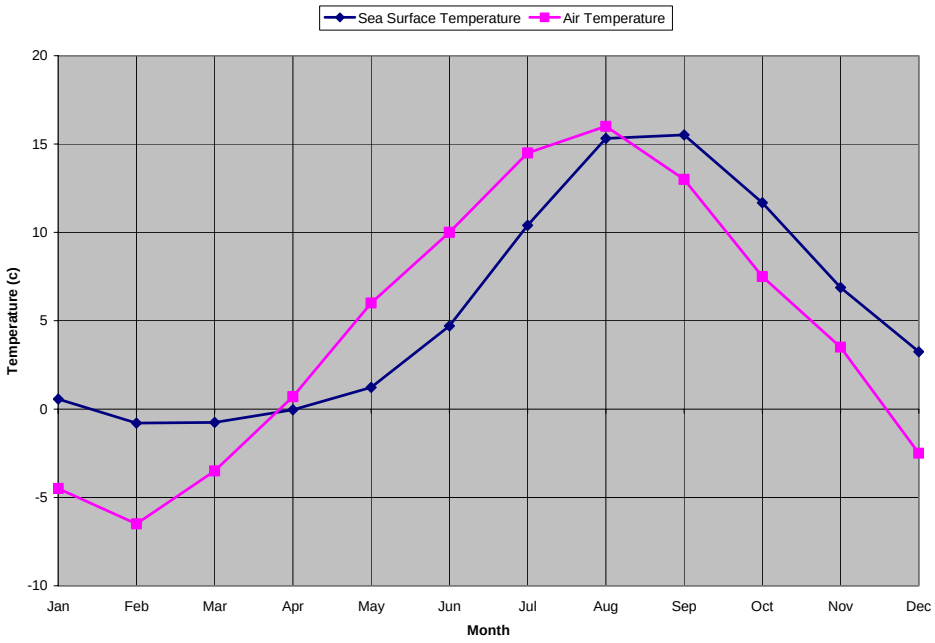

Source: SST field was derived from an analysis performed on **NOAA-JPL's AVHRR weekly 18km MCSST** dataset, using data from 1981 to 2000. Air temperatures were interpolated from the Environment Canada, Climatological Charts of the St. Lawrence.

Figure 2.17. Mean Sea Surface Temperature on the First Day of Each Month at Point 48.78°N 59.15°W and Mean Air Temperature for Each Month Near Grid Point 5817.

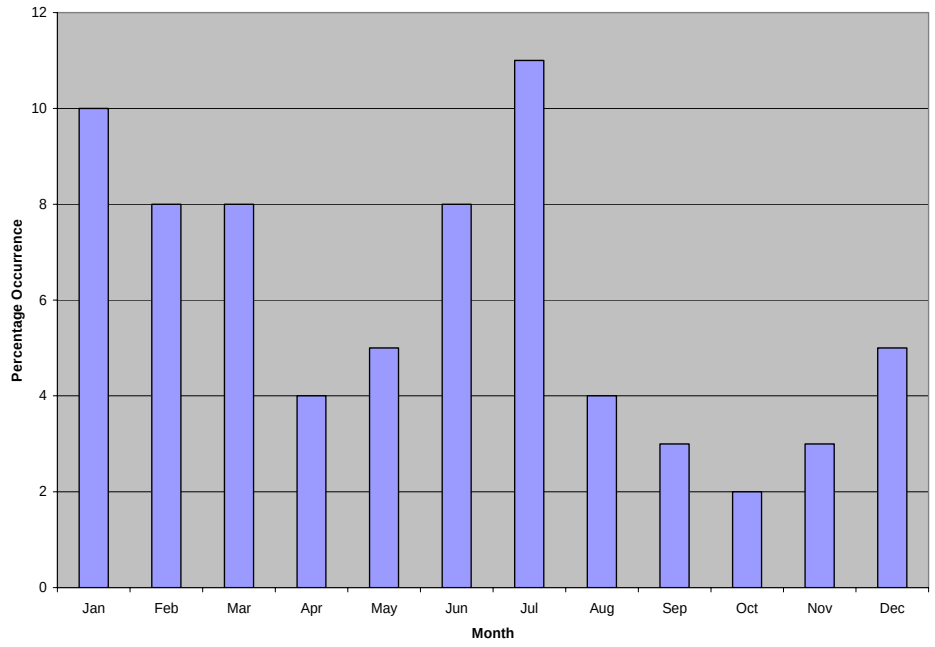

Source: Data was interpolated from the Environment Canada, Climatological Charts of the St. Lawrence.

Figure 2.18. Percentage Occurrence of Visibility Less Than 1 km for Each Month Near Grid Point 5817.

A sea state may be composed of the wind wave alone, swell alone, or the wind wave in combination with one or more swell groups. Swell energy may reach a point from more than two directions at a particular time. Swell wave energy reaching a point may have been generated within the local weather system or from within distant weather systems located elsewhere over the ocean. The former situation typically arises when a front, trough, or ridge crosses the point of concern, resulting in a marked wind shift.

Since the Study Area is a coastal region, swells here can only occur from an offshore direction. In this case, the offshore directions range from southwest to northeast, with reference to a clockwise system.

2.3.5 Wave Climate

The wave climate of the Gulf of St. Lawrence is dominated by extra-tropical storms that occur primarily during October to March period. Severe storms occasionally occur outside this period. Storms of tropical origin may occur during early summer, but most often between late-August and October. Hurricanes are usually reduced to tropical storm strength or evolve into extra tropical storms by the time they reach the Gulf of St. Lawrence. However, occasionally these storms retain hurricane force winds and subsequently produce high waves.

Based on mean values, the highest waves typically occur between October and January (Table 2.16). The maximum significant wave height of 9.43 m was recorded in January. Significant wave heights greater than 5 m occur in every month except for June, July and August. Figure 2.19 shows annual percentage exceedance curves of significant wave heights. Curves starting at less than 100% indicate the presence of ice.

In contrast, on the Grand Banks (grid point 5691) the maximum significant wave height was 13.7 m in February.

The spectral peak period of the waves varies seasonally. The typical peak period during summer is approximately four seconds (Table 2.17). In winter, the typical peak period is approximately six to seven seconds. A scatter diagram of the significant wave height versus spectral peak period is presented in Table 2.18.

It should be noted the wave climate as it relates to transformation from deep to shallow water may have to be examined in detail in site-specific EAs.

Table 2.16. Monthly Maximum, Mean and Standard Deviation of Significant Wave Height at Grid Point 5817.

Month	Maximum Height (m)	Standard Deviation (m)	Mean Height (m)
January	9.43	1.2	1.65
February	6.69	0.94	0.73
March	5.77	0.84	0.58
April	5.88	0.8	0.82
May	6.18	0.63	0.81
June	4.43	0.55	0.76
July	3.48	0.49	0.73
August	4.75	0.54	0.85
September	5.84	0.75	1.16
October	7.78	0.86	1.46
November	8.15	1.04	1.73
December	9.38	1.21	1.98

Source: AES grid point 5817. Lat 48.75°N, Long 59.17°W, 1954 to 2003.

Table 2.17. Percentage Occurrence of Peak Spectral Wave Period, Grid Point 5817.

	Peak Spectral Period (seconds)																	Total
Month	1	2	3	4	5	6	7	8	9	10	11	12	13	14	15	16	17	Obs
January	0.02	0.23	2.04	13.12	22.63	23.82	19.70	10.27	5.25	2.06	0.70	0.16						5580
February	0.28	2.75	5.37	23.73	27.71	19.46	12.80	4.80	2.02	0.95	0.06	0.06						3165
March	0.84	3.03	7.16	23.64	28.88	18.22	11.97	3.87	1.58	0.67	0.13	0.00						2974
April	0.97	3.74	6.86	28.07	28.35	17.93	9.90	3.04	1.06	0.09								4546
May	2.04	5.59	8.87	32.72	28.36	13.99	6.55	1.53	0.25	0.07	0.03							5941
June	2.16	6.45	9.12	32.27	31.50	13.15	4.08	1.16	0.12									5879
July	1.12	5.23	9.61	37.16	30.02	12.13	4.21	0.48	0.03									6076
August	0.41	3.65	6.90	33.77	33.05	15.24	5.83	0.92	0.15	0.08								6076
September	0.65	1.90	3.69	23.88	31.00	21.04	12.91	3.62	1.17	0.14								5880
October	0.03	0.44	1.97	15.54	27.70	25.53	18.24	7.21	2.53	0.76	0.03	0.02						6076
November		0.17	1.46	12.06	23.08	24.39	21.29	9.91	5.44	1.75	0.43	0.02						5880
December		0.18	0.74	8.71	19.54	23.24	23.62	12.69	7.24	2.52	1.22	0.28	0.03					6076

(Periods are rounded off to the nearest whole number.)

Source: AES grid point 5817. Lat 48.75°N, Long 59.17°W, 1954 to 2003.

Table 2.18. Percent Occurrence of Peak Wave Period against Significant Wave Height for Grid Point 5817.

	Wave Height (m)																Total
Period	0	1	2	3	4	5	6	7	8	9	10	11	12	13	14	15	
0	10.394																10.394
1	0.641																0.641
2	2.474																2.474
3	4.170	0.500															4.670
4	8.553	12.666	0.013														21.231
5	2.192	21.678	0.865														24.735
6	0.018	9.059	7.955	0.014													17.046
7		1.510	7.681	2.125	0.003												11.319
8	0.004	0.022	0.961	3.044	0.476												4.508
9	0.003		0.038	0.559	1.260	0.191											2.051
10	0.004			0.014	0.169	0.418	0.073	0.004									0.682
11				0.001	0.003	0.039	0.078	0.067	0.018								0.207
12							0.001	0.007	0.018	0.015							0.042
13										0.003							0.003
14																	
15																	
16																	
17																	
18																	
	28.453	45.435	17.51	5.757	1.911	0.648	0.152	0.078	0.036	0.018							100

Zero period and wave height represents when the grid point is "iced out"
(Wave Heights and Periods are rounded off to the nearest whole number.)

Source: AES grid point 5817. Lat 48.75°N, Long 59.17°W, 1954 to 2003.

2.4 Physical Oceanography

The Gulf of St. Lawrence is a highly stratified semi-enclosed sea with an approximate surface area of 226,000 km^2 (Koitutonsky and Bugden 1991). It exchanges salt with the North Atlantic Ocean and receives considerable input of fresh water from the St. Lawrence River and lesser amounts from other rivers. As a consequence, the Gulf of St. Lawrence acts like a large estuary where Coriolis effects (from force generated by the earth's rotation), geostrophic currents, baroclinic processes, formation of eddies, and wind stress effects are all important. The St. Lawrence River flowing into the Gulf of St. Lawrence drains an extensive watershed which reaches as far west as the Great Lakes.

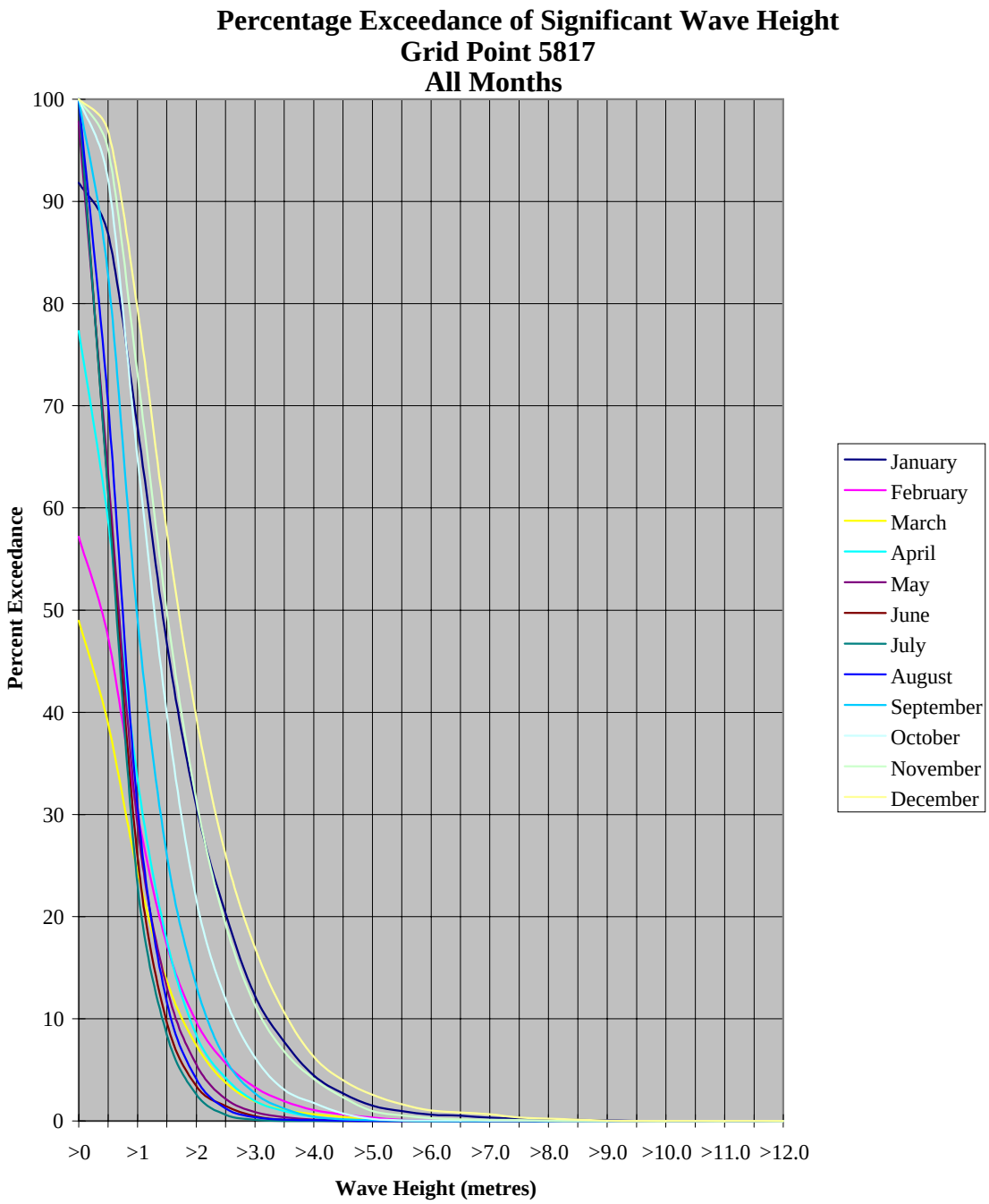

Source: AES grid point 5817. Lat 48.75°N, Long 59.17°W , 1954 to 2003.

Figure 2.19. Annual Exceedance of Wave height, Grid Point 5817.

2.4.1 Temperature and Salinity

A surface layer of relatively low salinities and seasonally variable thickness is a distinctive element of the water in the Gulf of St. Lawrence. The Study Area falls within North Atlantic Fishery Organization (NAFO) Division 4R and Unit Areas 4Ra, 4Rb, 4Rc and 4Rd. (see Figure 1.1). The seasonal temperature oscillations for this area are wide and increase slightly toward the south from 4Rb to 4Rd. In 4Rb, the range of temperature oscillations is over 15ºC while in 4Rd it is somewhat over 16ºC (Figure 2.20). During the summer, this temperature range decreases significantly with depth in the upper waters due to the presence of a cold intermediate layer between approximately 50 and 200 m. The cold water is due to the influx of Labrador Current water through the Strait of Belle Isle. Below 200 m, the temperature is in the range of 4°C to 6°C. In winter, the upper layer cools to below 0°C and becomes a nearly homogenous mixed layer.

Figure 2.21 shows average vertical distributions of winter and summer temperatures for NAFO Division 4R, taken from B.I.O.'s System Polygons hydrographic database.

2.4.2 Currents

The circulation in the Gulf of St. Lawrence is forced by several factors that include the following: tides, local and regional meteorological events, freshwater runoff, and water exchange through the Strait of Belle Isle and Cabot Strait. In general, the circulation near the surface is cyclonic (i.e., counter-clockwise) (Figure 2.22). The similarities between this cyclonic circulation pattern and the surface salinity distributions in the Gaspé and Magdalen Shallows regions indicate that the surface currents are a result of the geostrophic balance between the horizontal pressure gradient field, and Coriolis effects. (Koutitonsky and Bugden 1991). A feature of the circulation of the Gulf of St. Lawrence is a strong coastal current (Gaspé Current) which originates in the St. Lawrence River Estuary. This current divides into two branches: (1) a branch which crosses the Magdalen Shallows before exiting the Gulf on the southern side of Cabot Strait, and (2) a branch which follows the slope of the Laurentian Channel. The two connections with the Atlantic Ocean (Cabot Strait and Strait of Belle Island) reflect an estuarine-like circulation where fresh water flows to the ocean in the upper waters and more saline waters enter the Gulf in the deeper layers. The mean flushing time of fresh water in the Gulf of St. Lawrence is thought to be around six to eight months (Trites 1972).

The currents in Cabot Strait are the major avenues for water exchange between the Gulf of St. Lawrence and the Atlantic Ocean. In Cabot Strait a two-layer current structure is thought to exist with fresher water leaving the Gulf near the surface and saltier, heavier water entering the Gulf at depth. The surface outflow is shifted toward Cape Breton and the deeper inflow reaches the surface close to the southern shore of Newfoundland (El-Sabh 1976).

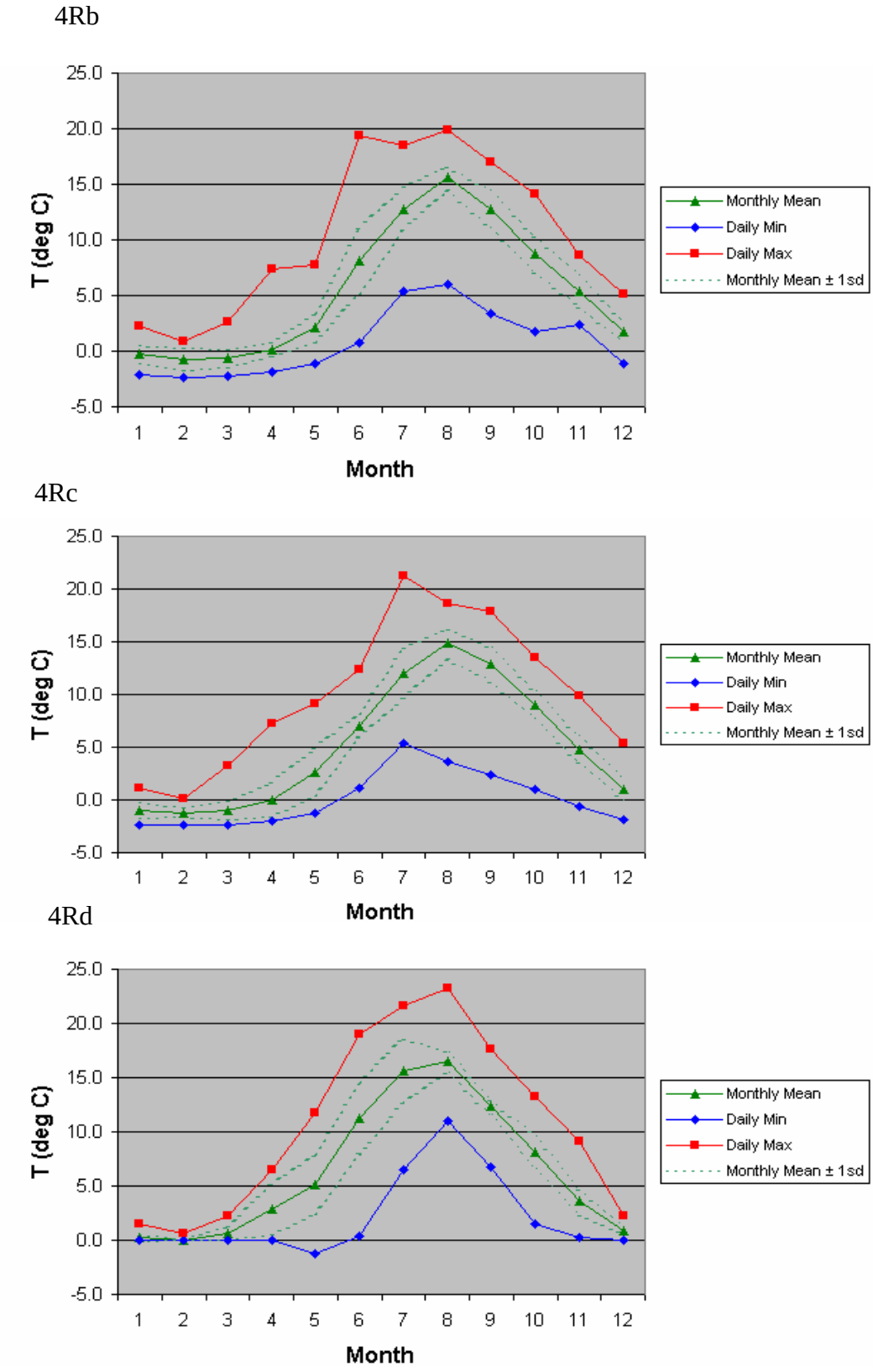

Figure 2.20. Seasonal Temperature Cycle for NAFO Division 4R Unit Areas.

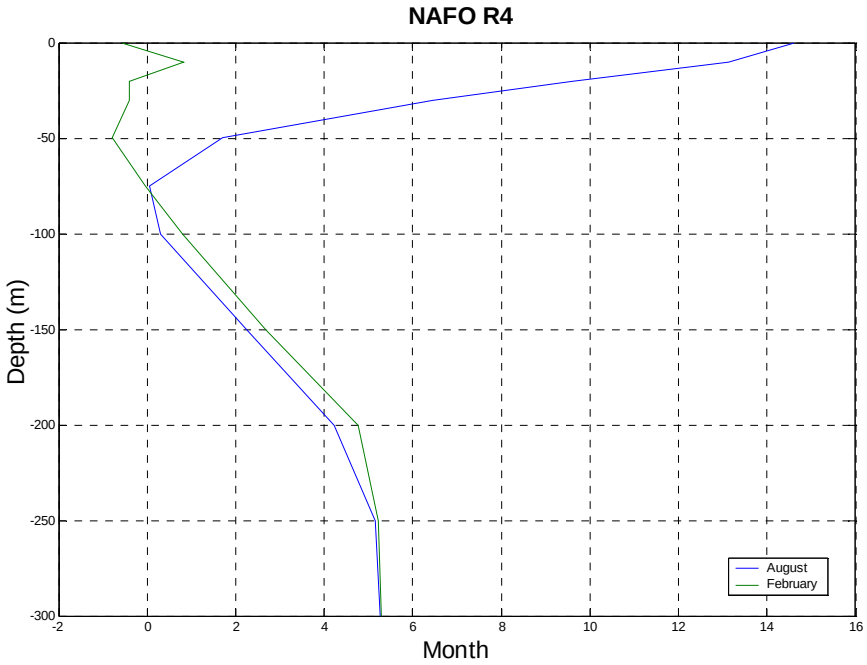

Figure 2.21. Average Vertical Temperature Distribution in NAFO area 4R in February and August. Data from B.I.O. System Polygons, Hydrographic Database.

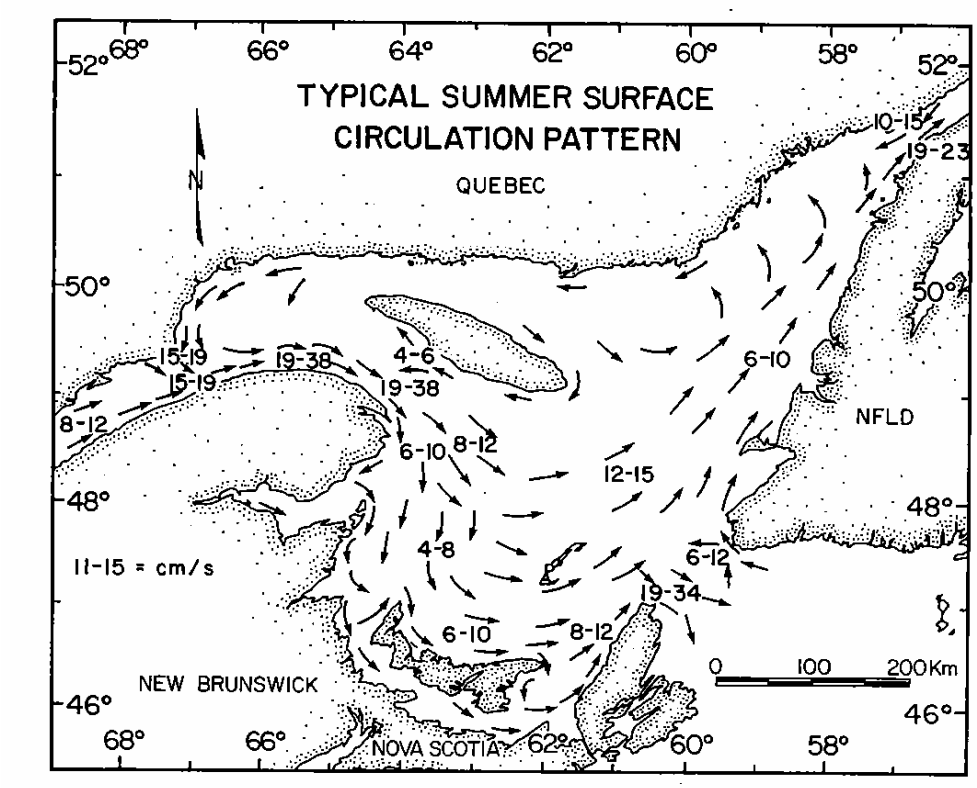

Source: Trites 1972 (Current speed ranges are given in cm/sec).

Figure 2.22. Summer Surface Circulation in the Gulf of St. Lawrence.

The circulation in the Strait of Belle Isle is into the Gulf along the Labrador side of the Strait and out of the Gulf along the Newfoundland side. However, episodic events of massive inflow and outflow though the whole Strait have been observed and are believed to be related to large scale barometric oscillations and the effect of winds.

The tides in the Gulf of St. Lawrence are dominated by the semi-diurnal M_2 constituent of 12.4 hours in the northeast sector of the Gulf of St. Lawrence and mixed in the centre of the Gulf (Godin 1979). The phases and amplitudes of the M_2 component of the tides are shown in Figure 2.23. The amplitudes of the M_2 constituent vary between 0.46 m and 0.53 m in the Study Area. With the exception of the St. Lawrence Estuary, these are the largest tides in the Gulf due to an amphidromic point being located near the Magdelen Islands. Tidal currents seldom exceed 30 cm/sec (Koutitonsky and Bugden 1991).

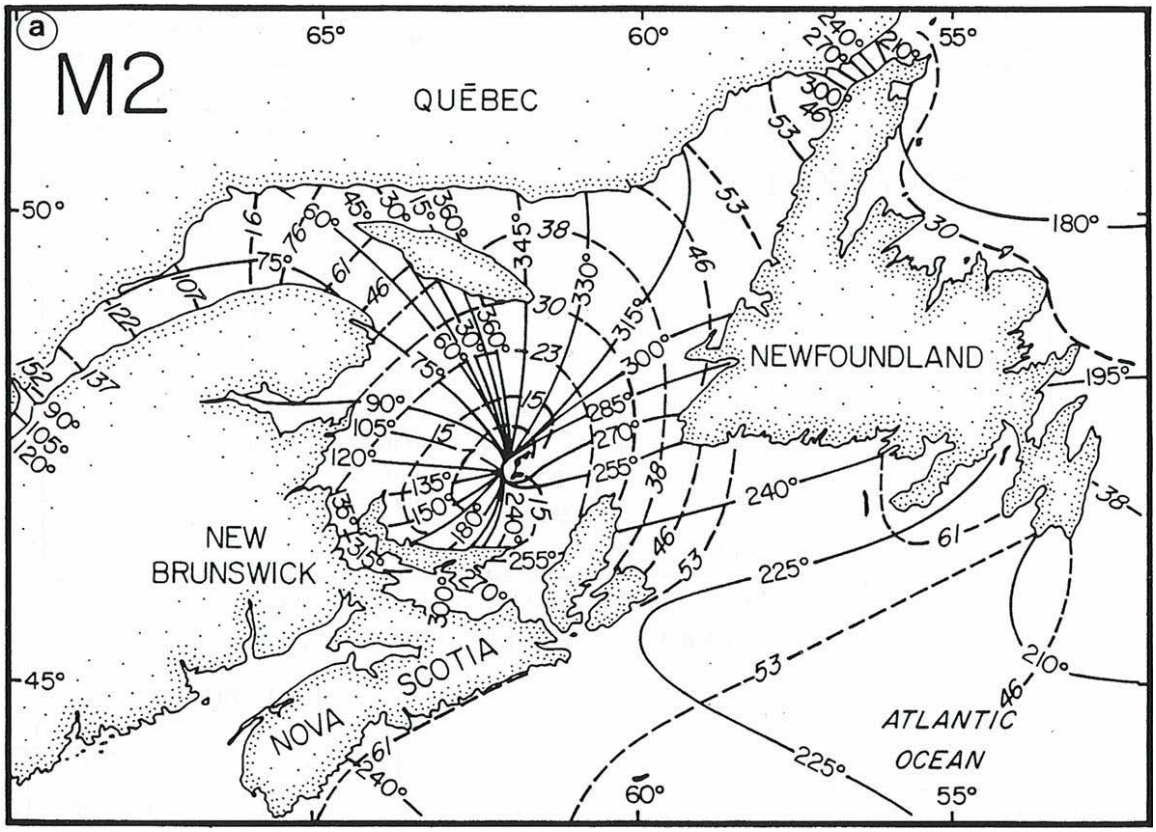

Source: Farquharson 1970. Amplitudes are in cm, and phases are relative to GMT zone.

Figure 2.23. Co-amplitude (dashed) and Co-phase (solid) Lines for the M_2 Tides in the Gulf of St. Lawrence.

Wind stress forcing is a major source of kinetic energy for the Gulf of St. Lawrence. From June to October, the winds are weak. Saunders (1977) estimated the mean seasonal wind stress values over the North Atlantic continental shelf, using wind observations from ships for the period 1941-1972 (Figure 2.24). In this Figure, a predominant westerly direction of the winds is observed during all seasons, with a notable northerly component in spring and a southerly component during the summer.
El-Sabh (1976) and Trites (1972) report northeastward residual currents along the western coast of Newfoundland, corresponding to the cyclonic character of the circulation patterns within the Gulf.

Currents off the southwestern coast of Newfoundland are, in general, the result of interaction between the waters entering the Gulf through Cabot Strait next to the Newfoundland coast, and the eastward flows in the central sector of the Gulf.

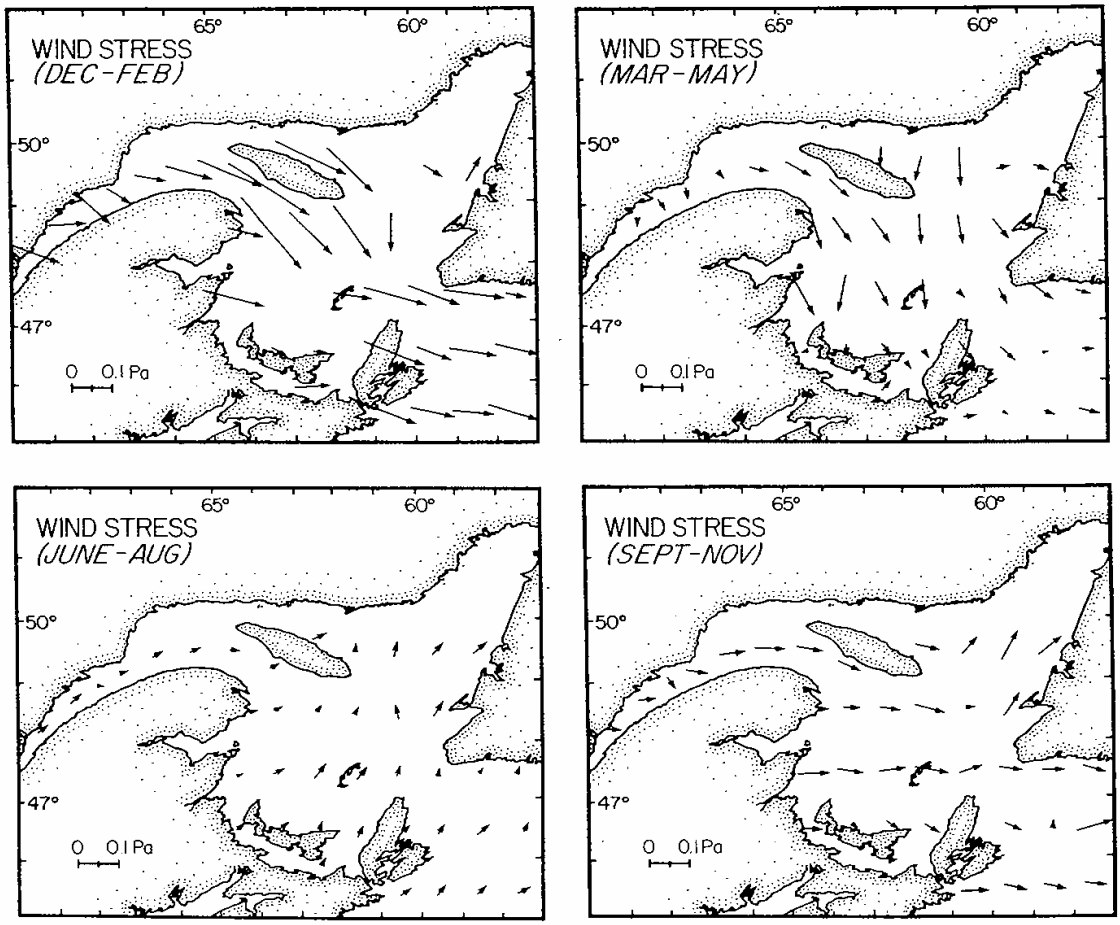

Source: Saunders (1977).

Figure 2.24. Mean Seasonal Wind Stress (1941-1972) over the Gulf of St. Lawrence, Averaged from Ship Observations.

According to El-Sabh (1976), the flow in the Study Area is usually directly northeastward along the west coast of Newfoundland. However, clockwise and anticlockwise gyres are part of the permanent features of the circulation pattern in the Gulf. These gyres sometimes move along with the general flow.

The presence of mesoscale and synoptic eddies off the western coast of Newfoundland is frequent and has been documented by means of numerical modeling (Koutitonksy and Bugden 1991), geostrophic calculations derived from oceanographic data (El-Sabh 1976), and direct current measurements (Trites 1972). The presence of these gyres suggests a very complex ocean circulation pattern in the Study Area (Figure 2.25).

Some moored current data exists for the Study Area from which current velocities can be examined. The information on ocean currents is concentrated around Rocky Harbour, St. George's Bay, and Port-aux-Basques. The locations are shown in Figure 2.26.

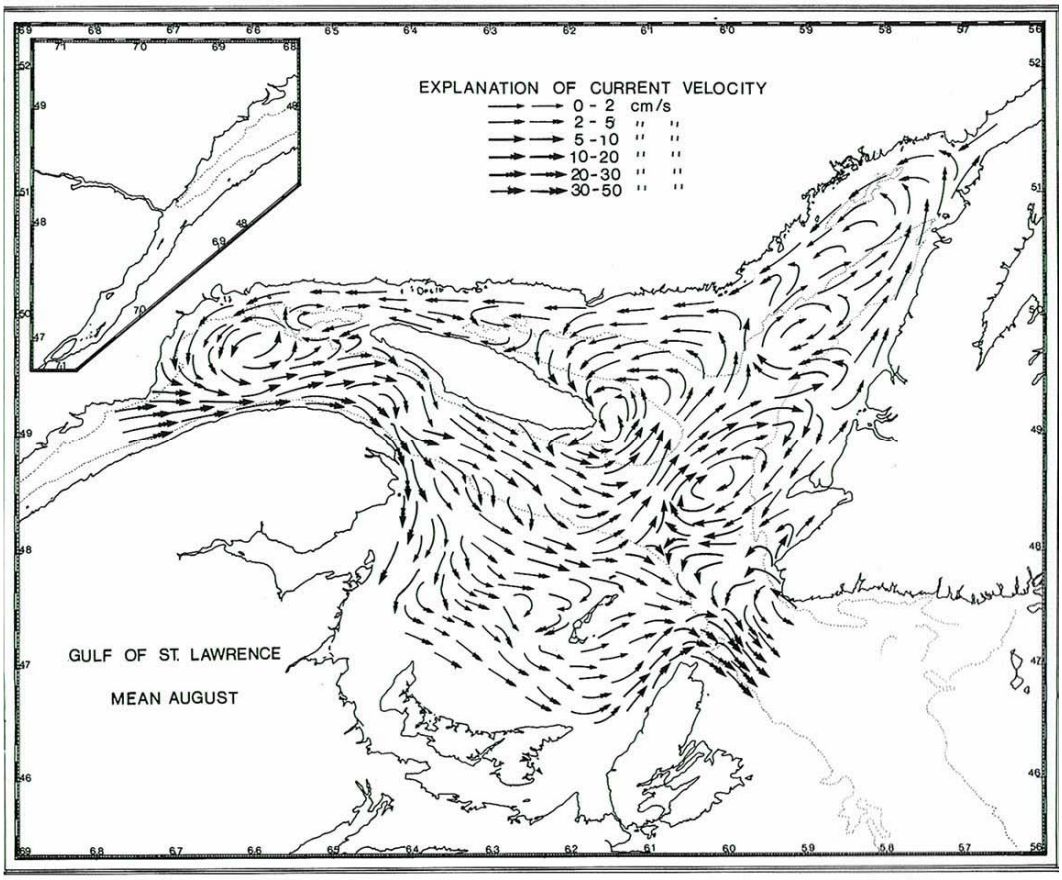

Figure 2.25. Field Surface of the Geostrophic Currents in the Gulf of St. Lawrence during August.

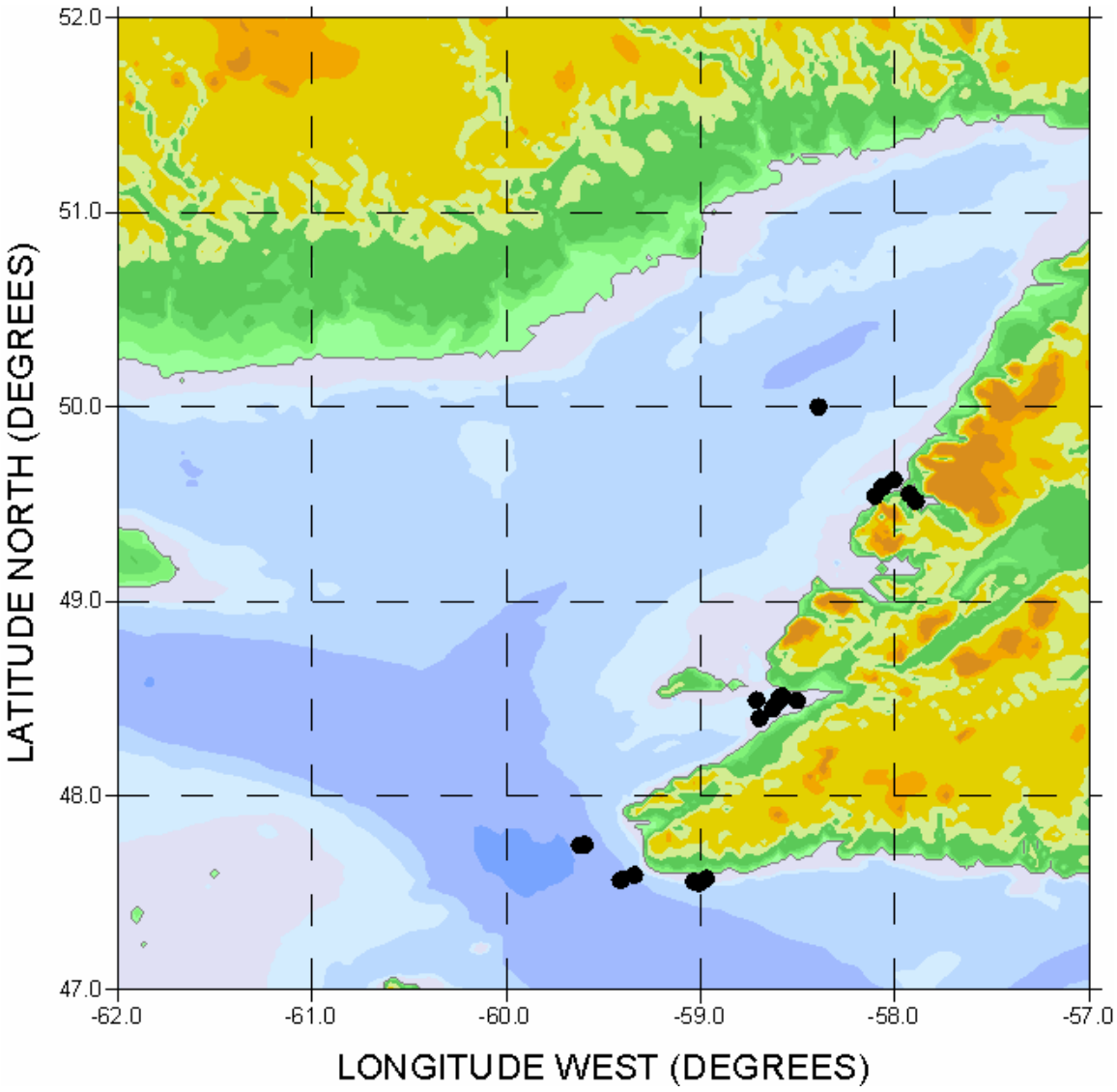

Figure 2.26. Locations of Moored Current Meter Data.

2.5 Ice Conditions

The area off the west coast of Newfoundland is subject to seasonal incursions of ice. There are considerable variabilities in spatial distribution, season length and source of ice between the northern and southern parts of the Study Area. The Study Area is primarily subjected to sea ice as opposed to icebergs but there have been isolated reports of icebergs in the northern and western boundaries of the Study Area.

C-CORE (2005) conducted analyses to determine an ice-free season during which the influence of iceberg and pack ice on ice-sensitive operations may be considered negligible for areas of offshore Newfoundland where exploration activities may potentially occur. The region considered included areas off the west coast of Newfoundland from Cape Anguille to St. Paul's Inlet (southern and central parts of the Study Area).

2.5.1 Data Sources

The primary sources of sea ice data for the Study Area are the Canadian Ice Services (CIS) database and the Sea Ice Climate Atlas, East Coast of Canada 1971-2000. The pack ice data used in C-CORE's analyses covered 36 years.

The primary sources of iceberg data are the International Ice Patrol Database, the CIS iceberg charts, the Provincial Aerospace Iceberg Database, and the PERD (2004) Iceberg Sighting Database. The PERD (2004) data were most extensive and were therefore considered most appropriate for the analysis. The iceberg data used in C-CORE's analyses covered 44 years.

2.5.2 Sea Ice

Sea ice cover in the Study Area comes from two primary sources: (1) sea ice formed off the coast of Labrador which drifts down through the Strait of Belle Isle to the northern part of the Study Area, and (2) ice that forms in the Gulf of St Laurence and affects the central and southern parts of the Study Area. All sea ice in the Study Area is first-year ice, ranging in its un-deformed thickness from 30 to 120 cm. Total ice coverage across the Study Area ranges from 100% in the northern and western sectors to 60% in the inshore areas. Pack ice was most important at Port au Port in establishing the duration of the ice-free season. Based on pack ice, the ice-free season for the Port au Port region was determined to be May to December (C-CORE 2005).

2.5.3 Season Length

There is a large variability in season length between the northern and southern sectors of the Study Area. Sea ice generally drifts across the northern boundary during the first week in January and reaches the southern boundary by the third week of February.

Maximum spatial coverage is typically reached by the second week of March when the entire Study Area is covered with sea ice (Figure 2.27). The sea ice clears the southern boundary by the first week of April and the Study Area is typically ice free by the second week of May. Total season length based on the 30-year median ice coverage is shown in Table 2.19.

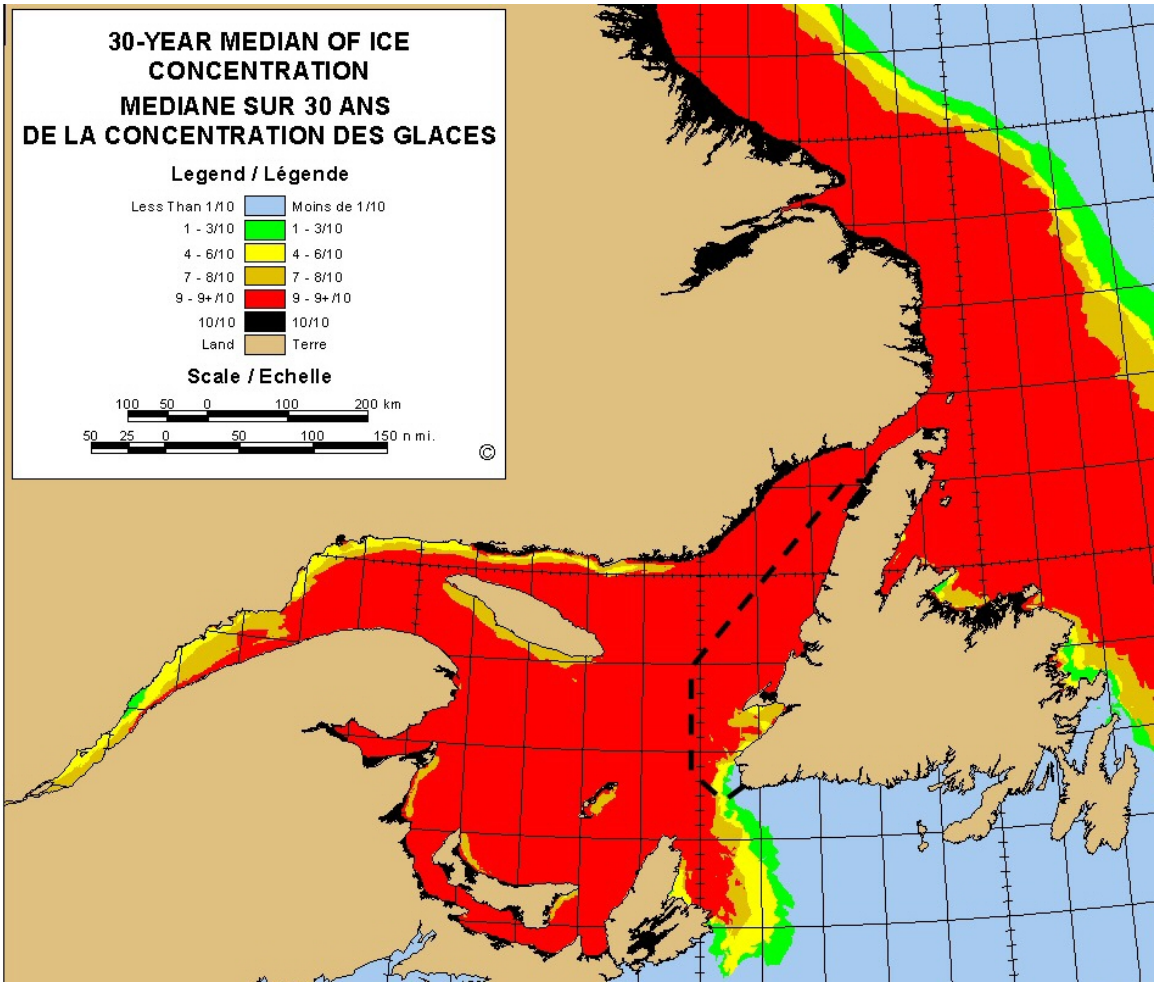

Figure 2.27. Maximum Pack Ice Extent in March (Study Area Delineated by Dashed Line).

Table 2.19. Ice Season Durations.

Sector	Freeze Up	Break Up	Total Days
Northern Sector	Jan-08	May-07	120
Southern Sector	Feb-19	April-02	43
Extreme Cover	Dec-11	July-16	217

2.5.4 Icebergs

The number of iceberg sightings in the Study Area are low. Normalized iceberg drift indicates that bergs travel down the Strait of Belle Isle and then follow the primary current along the Quebec shore of the Gulf.

Isolated iceberg sightings have been reported around the northern and western boundaries of the Study Area. However, there are few quantitative data on iceberg size, shape, or densities in this area.

Based on icebergs, the ice-free season for the Port au Port region was determined to be the entire year (C-CORE 2005). In the <150m waters off Bay of Islands and Gros Morne National Park, icebergs have been infrequently recorded between March and June during the 1960 to 2003 period. Pack ice, on the other hand, occurs in this same area between December and May, based on at least one observation in all years (1969 to 2004) (C-CORE 2005).

2.5.5 Icing of Superstructures

Icing of superstructures can occur throughout the NW Atlantic in winter, including the Gulf of St. Lawrence. Icing caused by freezing spray and freezing precipitation can influence personnel safety and vessel/rig stability. The degree of icing is influenced by a number of factors such superstructure design, air and water temperatures, wind conditions, amount and type of precipitation and other factors.

2.6 Planning Implications

The physical environment has direct implications for oil and gas activities because it may affect operations and safety. It also should be noted that the effects of the environment on a project must be considered pursuant to the requirements for an environmental assessment under the *Canadian Environmental Assessment Act* (*CEAA*).

The physical environment of the west coast is typically less harsh than the Grand Banks at least in terms of iceberg and wave conditions. At the same time, a number of physical factors which likely enhance the biodiversity of the Study Area may also increase the adverse effects of an accidental oil spill (see Section 4.3)

Planning implications related to the physical environment are summarized in the following sections.

2.6.1 Geology

The geology of the Study Area is, of course, of paramount interest to the oil industry as it determines the oil and gas potential. The Study Area is considered to have a relatively low seismic hazard with respect to peak horizontal ground accelerations and velocities and for relatively short term activities such as exploratory drilling. Nonetheless, in the event of a production development application, all potential geohazards, including seismic events, would likely have to be examined in more detail.

2.6.2 Bathymetry

Considering that water depths within the Study Area range from the low water mark of the intertidal zone to >500 m in the offshore, there is considerable diversity of the physical and biological environments, and hence of potential effects of oil and gas activities. This diversity is discussed in greater detail in the next section on the biological environment.

2.6.3 Currents

The currents in the Study Area are certainly of operational concern (e.g., effects of the environment on a project). In general, ocean currents in the somewhat enclosed Gulf of St. Lawrence flow in a counter-clockwise direction. This cyclonic flow could potentially be a factor in the effects of an accidental oil spill in the Study Area (see Section 4.3). Current meter data are typically collected during drilling operations as part of a physical environment monitoring program, thereby enhancing the physical database for the area. Currents play an important role in the distribution of eggs and larvae of fish and invertebrates.

2.6.4 Ice

Ice and icebergs are of paramount interest from an operational and safety point of view. Icebergs are less of an issue in the Study Area compared to areas off eastern Newfoundland and Labrador. In terms of ice, sea ice plays a dominant role in the Study Area. For example, sustained westerly winds have a tendency to pile up ice on the west coast which can hamper coastal operations. [It should be noted that daily ice charts for the Gulf of St. Lawrence are available from the CIS.]

Sea ice is also a factor in the shaping of shallow water plant and animal communities, and it affects oil and gas industry-related issues that include underwater sound transmission, spill behaviour, and spill remediation (see Section 4.3). Icing of superstructures can have implications for the safety of both personnel and offshore vessels and structures.

2.6.5 Climatology, Winds, Waves, Temperature, and Salinity

These physical variables are all of concern to operations and safety. Winds, for example, blow predominantly onshore along western Newfoundland, which would be of concern in the case of an accidental oil spill (see Section 4.3). Data on these variables are typically included in site-specific EAs. These physical factors are also involved in the shaping of shallow water plant and animal communities. Operators will be required to collect meteorological and oceanographic data to support operations.